

NASA-CR-170,276

NASA-CR-170276
19830015887

STRESS DISTRIBUTION IN BONDED JOINTS

by

F. Erdogan and M. Ratwani

Lehigh University
Bethlehem, Pennsylvania



October 1970

NF02078

STRESS DISTRIBUTION IN BONDED JOINTS

by

F. Erdogan and M. Ratwani

Prepared under Grant No. NGR-39-007-011 for
National Aeronautics and Space Administration

Lehigh University
Bethlehem, Pennsylvania

October 1970

N83-74736

"STRESS DISTRIBUTION IN BONDED JOINTS"

by

F. Erdogan and M. Ratwanı

SUMMARY

The stress distribution in plates and tubes bonded through stepped joints is analyzed. The problem is solved under the assumption of generalized plane stress. Two numerical examples are worked out on specific plate and tube geometries and a material combination of aluminum vs. boron-epoxy composite. The effect of step ends is separately studied. As a limiting case, the solution for bonded plates with smoothly tapered joints is also given.

SYMBOLS

$a_{1j}, a_{2j}, \alpha_j, \beta_j$	constants defined in the text
A_j, B_j	integration constants
d_j	thickness of the adhesive at the jth step end
E_1, ν_1	elastic constants for the isotropic medium
$E_{2x}, E_{2z} (E_{2\theta})$	} elastic constants for the orthotropic medium
$\nu_{2x}, \nu_{2z} (\nu_{2\theta}), G_2$	
E_3, G_3, ν_3	elastic constants of the adhesive

h_1, h_{1j}	thicknesses for the isotropic medium
h_2, h_{2j}	thicknesses for the orthotropic medium
h_3	thickness of the adhesive
K_j	total tensile force acting on the j th step end
$L = \ell_{j+1} - \ell_j$	step length
ℓ_j	distance of the j th step from the origin $x = 0$
$p(x), q(x)$	contact stresses in smoothly tapered joint
P_0	total load (in tubes, and per unit width in plates)
$P_{1j}(x), P_{2j}(x)$	total loads in media 1 and 2
r, θ, x	cylindrical coordinates (in tubes)
r_{1j}^o, r_{1j}^i	outer and inner radii in stepped aluminum tube
r_{2j}^o, r_{2j}^i	outer and inner radii in boron-epoxy tube
S_{1j}, S_{2j}	cross-sectional areas of the tubes
u_{1i}, u_{2i}	displacements in media 1 and 2
x, y, z	rectangular coordinates
$\epsilon_{1k}, \epsilon_{2k}$	components of strain ($k = x, y, z$ or r, θ, x)
σ_{1k}, σ_{2k}	components of stress ($k = x, y, z$ or r, θ, x)

τ_j	contact shear in stepped joint
α	angle of contact in tapered joint
$\phi(x)$	total tensile load in material 2 for the tapered joint

1. INTRODUCTION

The main purpose of this study is to develop a model for the calculation in stresses in bonded overlapped joints in plates and tubes. In a previous study on reinforcing cover plates bonded to an elastic base plate, it was shown that if the adhesive layer is not taken into account as a third medium, the load transfer between the two plates takes place along the boundary of the bond area only [1]. It was also shown that a more realistic solution of the problem can be obtained if one considers the adhesive layer as a third elastic medium acting basically as a shear spring between the two plates. In this study this concept will be used to analyze the stresses in the stepped joints between aluminum and boron-epoxy plates and tubes. The particular configurations studied are shown in Figures 1 and 2.

2. PLATES BONDED THROUGH A STEPPED JOINT

Let an isotropic plate, 1, be bonded to an orthotropic plate, 2, through a stepped joint as shown in Figure 1. The problem is that of determining the stresses $\sigma_{1x}(x)$ and $\sigma_{2x}(x)$ in the plates and the shear stress $\tau(x)$ on the interface

under a uniform tensile force p_0 applied to the plates away from the joint. The problem will be solved under the following approximating assumptions:

a) The thicknesses h_1 , h_{1j} , h_2 , h_{2j} and h_3 are small compared to the other dimensions of the composite structure so that the individual layers and the composite plate may be considered to be under generalized plane stress (i.e., $\sigma_{1y} = 0 = \sigma_{2y}$).

b) The thickness variation of the stresses in the plates will be neglected under the usual assumption that the surface shear transmitted through the adhesive layer acts as a body force.

c) In z direction (see Figure 1), it will be assumed that either $\bar{\epsilon}_z = \epsilon_{1z} = \epsilon_{2z} = 0$ or $\bar{\sigma}_z = 0$, $\bar{\sigma}_z$ being the average stress in the composite*.

For the i th portion of the stepped joint (i.e., $l_i < x < l_{i+1}$), let h_{1i} , h_{2i} and h_3 be the thicknesses, $p_{1i}(x)$ and $p_{2i}(x)$ be the resultant forces per unit width acting in x direction, $u_{1i}(x)$ and $u_{2i}(x)$ be the displacements in x direction, and $\tau_i(x)$ be the adhesive shear stress. Neglecting the adhesive forces acting on the $x = l_i$ parts of

* The first refers to wide plates under "fixed grip" type of loading. In the second the loads are applied to the plates at locations sufficiently far from the joint and the sides $z = \text{constant}$ are traction-free.

the steps (such as AB in Figure 1), from the equilibrium of the plate 2 and the adhesive layer we obtain

$$p_{2i}(x) = p_{2i-1}(l_{i-1}) + \int_{l_{i-1}}^x \tau_i(x) dx, \quad (i = 1, \dots, n) \quad (1)$$

$$\tau_i(x) = \frac{G_3}{h_3} (u_{2i} - u_{1i}), \quad (i = 1, \dots, n) \quad (2)$$

where G_3 is the shear modulus of the adhesive. It is assumed that the materials of plate 1 is isotropic with constants E_1 , ν_1 and plate 2 is orthotropic with constants E_{2x} , ν_{2x} , E_{2z} , ν_{2z} , G_2 .

$$a) \quad \bar{\epsilon}_z = \epsilon_{1z} = \epsilon_{2z} = 0$$

Under this assumption $\sigma_{1z} = \nu_1 \sigma_{1x}$, $\sigma_{2z} = \nu_z \sigma_{2x}$ and from the stress-strain relations (with $\sigma_{1y} = 0 = \sigma_{2y}$) and

$$p_{1i} = p_0 - p_{2i}, \quad \sigma_{1x} = \frac{p_{1i}}{h_{1i}}, \quad \sigma_{2x} = \frac{p_{2i}}{h_{2i}} \quad (3)$$

we obtain

$$\begin{aligned} \epsilon_{1x}(x) &= \frac{1-\nu_1^2}{E_1 h_{1i}} [p_0 - p_{2i}(x)] \\ \epsilon_{2x}(x) &= \frac{1-\nu_{2x}\nu_{2z}}{E_{2x} h_{2i}} p_{2i}(x) \end{aligned} \quad (4)$$

Noting that

$$\epsilon_{1x} = \frac{du_{1i}}{dx}, \quad \epsilon_{2x} = \frac{du_{2i}}{dx} \quad (5)$$

from (1), (2) and (4) we obtain

$$\frac{d^2}{dx^2} p_{2i} - \alpha_i^2 p_{2i} = \beta_i p_0, \quad (i = 1, \dots, n) \quad (6)$$

where n is the number of steps and

$$\alpha_i^2 = \frac{\mu_3}{h_3} \left[\frac{1-\nu_1^2}{E_1 h_{1i}} + \frac{1-\nu_{2x}\nu_{2z}}{E_{2x} h_{2j}} \right] \quad (7)$$

$$\beta_i = - \frac{\mu_3}{h_3} \frac{1-\nu_1^2}{E_1 h_{1i}}$$

$$b) \quad \bar{\sigma}_z = 0$$

In this case we have

$$h_{1i} \sigma_{1z} + h_{2i} \sigma_{2z} = 0, \quad \epsilon_{1z} = \epsilon_{2z} \quad (8)$$

Using (8) and the stress-strain relations with $\sigma_{1y} = 0 = \sigma_{2y}$ we obtain

$$\epsilon_{1x}(x) = \frac{1}{E_1 h_{1i}} [p_0 (1-\nu_1 a_{2i}) - (1-\nu_1 a_{1i}) p_{2i}(x)] \quad (9)$$

$$\epsilon_{2x}(x) = \frac{1}{E_{2x} h_{2i}} [p_0 \nu_{2x} a_{2i} + (1-\nu_{2x} a_{1i}) p_{2i}(x)]$$

where

$$a_{1i} = (v_1 + v_{2z} \frac{E_1 h_{1i}}{E_{2z} h_{2i}}) / (1 + \frac{E_1 h_{1i}}{E_{2z} h_{2i}}) \quad (10)$$

$$a_{2i} = v_1 / (1 + \frac{E_1 h_{1i}}{E_{2z} h_{2i}})$$

From equations (1), (2), (5) and (9) we again obtain the differential equation (6) for which the constants α_i and β_i are given by

$$\alpha_i^2 = \frac{\mu_3}{h_3} \left(\frac{1-v_{2x} a_{1i}}{E_{2x} h_{2i}} + \frac{1-v_1 a_{1i}}{E_1 h_{1i}} \right) \quad (11)$$

$$\beta_i = \frac{\mu_3}{h_3} \left(\frac{v_{2x} a_{2i}}{E_{2x} h_{2i}} - \frac{1-v_1 a_{2i}}{E_1 h_{1i}} \right)$$

After solving (6) for $p_{2i}(x)$, the stresses in x direction in the plates 1 and 2, and the interface shear may be obtained from

$$\sigma_{1xi}(x) = \frac{1}{h_{1i}} [p_0 - p_{2i}(x)], \quad \sigma_{2xi}(x) = \frac{1}{h_{2i}} p_{2i}(x) \quad (12)$$

$$\tau_1(x) = \frac{d}{dx} p_{2i}(x)$$

The solution of the differential equation (6) may be written as

$$p_{2i}(x) = A_i e^{-\alpha_i x} + B_i e^{\alpha_i x} - \frac{\beta_i p_0}{\alpha_i^2}, \quad (i = 1, \dots, n) \quad (13)$$

The $2n$ integration constants A_i, B_i are determined from the following $2n$ conditions*

$$\begin{aligned} p_{21}(0) &= 0, \quad p_{2n}(l_n) = p_0 \\ p_{2i}(l_i) &= p_{2i+1}(l_i), \quad i = 1, \dots, n-1 \\ \frac{d}{dx} p_{2i}(l_i) &= \frac{d}{dx} p_{2i+1}(l_i), \quad i = 1, \dots, n-1 \end{aligned} \quad (14)$$

3. REINFORCED TUBE UNDER AXIAL LOAD

The configuration for this axially symmetric problem is shown in Figure 2. The problem is quite similar to that discussed in Section 2b. It is solved here under the assumption that the thickness of the composite tube is sufficiently small compared to its radii to justify the assumptions that a) the radial stress σ_r is negligible, and b) the r -dependence of the stresses may be ignored.

In this case, assuming that p_0, p_{1j}, p_{2j} stand for the total axial loads in, respectively, the composite, the isotropic (inner) tube, and the orthotropic reinforcing shell, we find

*The last set of equations in (14) follows from (2), third equation in (12) and the continuity of the displacements at $x = l_i$, namely $u_{2i}(l_i) - u_{1i}(l_i) = u_{2i+1}(l_i) - u_{1i+1}(l_i)$.

$$\frac{d^2}{dx^2} p_{2j}(x) - \alpha_j^2 p_{2j}(x) = \beta_j p_0, \quad (j = 1, \dots, n) \quad (15)$$

where

$$\alpha_j^2 = \frac{\mu_3}{h_3} \left[\frac{1}{E_{2x}} \left(\frac{1}{s_{2j}} - \frac{\nu_{2x} a_{1j}}{h_{2j}} \right) + \frac{1}{E_1} \left(\frac{1}{s_{1j}} - \frac{\nu_1 a_{1j}}{h_{1j}} \right) \right]$$

$$\beta_j = \frac{\mu_3}{h_3} \left[\frac{\nu_{2x} a_{2j}}{E_{2x} h_{2j}} - \frac{1}{E_1} \left(\frac{1}{s_{1j}} - \frac{\nu_1 a_{2j}}{h_{1j}} \right) \right]$$

$$a_{1j} = \left(\frac{\nu_1}{E_1 s_{1j}} + \frac{\nu_{2\theta}}{E_{2\theta} s_{2j}} \right) / \left(\frac{1}{E_1 h_{1j}} + \frac{1}{E_{2\theta} h_{2j}} \right)$$

$$a_{2j} = \left(\frac{\nu_1}{E_1 s_{1j}} \right) / \left(\frac{1}{E_1 h_{1j}} + \frac{1}{E_{2\theta} h_{2j}} \right)$$

In the tube problem $x = \ell_n$ is a plane of symmetry. Thus, in solving the differential equations (15), the only change in the boundary conditions (14) will be to change the condition at $x = \ell_n$ from $p_{2n}(\ell_n) = p_0$ to

$$\frac{d}{dx} p_{2n}(\ell_n) = 0 \quad (16)$$

4. EFFECT OF STEP ENDS

In the foregoing analysis the effect of the step ends (such as AB in Figure 1) was neglected by assuming that these surfaces $x = \ell_i$, ($i = 0, \dots, n$) are traction-free. However, these effects can easily be introduced into the analysis by assuming that the adhesive layer at $x = \ell_i$ acts as a tension spring. Defining the total contact loads in x direction

acting on the steps $x = \ell_i$ ($i = 0, 1, \dots, n$) by K_i , the equilibrium equation (1) may be modified as

$$p_{2i}(x) = p_{2i-1}(\ell_{i-1}) + \int_{\ell_{i-1}}^x \tau_i(x) dx + K_{i-1} \quad (i = 1, \dots, n) \quad (17)$$

From the derivation of the differential equation (6) it is easily seen that (6) will remain valid with the same coefficients α_i and β_i . However, there are $n+1$ new unknown constants K_i . The additional conditions to account for these constants are obtained by considering the equilibrium of the adhesive layers at $x = \ell_i$, ($i = 0, 1, \dots, n$). For example, at $x = \ell_i$ we may write

$$\begin{aligned} \epsilon_3 &= \frac{1-\nu_3^2}{E_3} \frac{K_i}{h_{i+1}-h_i} = \frac{u_2(\ell_i) - u_1(\ell_i)}{d_i} = \frac{h_3}{G_3 d_i} \tau_i(\ell_i) \\ &= \frac{h_3}{G_3 d_i} \frac{d}{dx} p_{2i}(\ell_i) \end{aligned} \quad (18)$$

Thus the boundary conditions for this problem in bonded plates become

$$\begin{aligned} p_{21}(0) &= K_0, \quad p_{2n}(\ell_n) = p_0 - K_n \\ p_{2i+1}(\ell_i) &= p_{2i}(\ell_i) + K_i, \quad (i = 1, \dots, n-1) \\ \frac{d}{dx} p_{2i+1}(\ell_i) &= \frac{d}{dx} p_{2i}(\ell_i), \quad (i = 1, \dots, n-1) \\ \frac{d}{dx} p_{2i}(\ell_i) &= \frac{(1-\nu_3)d_1}{2h_3(h_{i+1}-h_i)} K_i, \quad (i = 0, 1, \dots, n) \end{aligned} \quad (19)$$

with $h_{20} = 0$. Equations (19) replace (14) in solving (6). Similar conditions can be derived for the reinforced tube.

5. SMOOTHLY TAPERED JOINT

Let the two plates be bonded through a smoothly tapered joint as shown in Figure 3. This is the limiting case of the configuration given in Figure 1 in which $n \rightarrow \infty$ while $\tan\alpha = (h_{2i+1} - h_{2i})/(\ell_{i+1} - \ell_i)$ remains constant. In this section the solution of this problem will be given under the restrictive assumptions that, a) the thicknesses h_1, h_2 are very small compared to other dimensions of the plate, so that the generalized plane stress assumption is valid for the plates as well as their tapered parts, b) $\sigma_{1y} = 0 = \sigma_{2y}$ throughout the plates, c) the contact stresses act on the tapered parts of the plates as body forces, d) through-the-thickness distribution of the stresses are negligible, and e) the adhesive acts as a combination of shear and tension springs.

Let h_3 be the thickness, G_3, E_3 be the elastic constants of the adhesive layer, $p(x)$ and $q(x)$ be the normal and shear components of the contact force, and $\phi(x)$ be the total force (per unit width) acting on the plate 2 (see Figure 3). From the equilibrium of plate 2 we find (Figure 3b)

$$\phi(x) = \int_0^x (p(t)\sin\alpha + q(t)\cos\alpha) \frac{dt}{\cos\alpha} \quad (20)$$

$$\int_0^x (p(t)\cos\alpha - q(t)\sin\alpha) \frac{dt}{\cos\alpha} = 0, \quad (0 < x < \ell)$$

Since the second equation of (20) is valid for all x in $0 < x < l$, we have

$$p(t)\cos\alpha = q(t)\sin\alpha \quad (21)$$

and (20) becomes

$$\phi(x) = (1 + \tan^2\alpha) \int_0^x q(t)dt \quad (22)$$

Now let the total relative displacement vector (at point t) be $\Delta\vec{u}$, with normal and tangential components Δu_n , Δu_t and x , y components Δu_x , Δu_y (Figure 3c). From the equilibrium of the adhesive we may write

$$\Delta u_n = \frac{h_3}{E_3} p(x), \quad \Delta u_t = \frac{h_3}{G_3} q(x) \quad (23)$$

Using (21) and (23), from Figure 3c, it follows that

$$u_{2x} - u_{1x} = \Delta u_x = h_3 \left(\frac{1}{G_3} + \frac{\tan^2\alpha}{E_3} \right) q(x) \cos\alpha \quad (24)$$

Thus, assuming $\bar{\epsilon}_z = \epsilon_{1z} = \epsilon_{2z} = 0$, and observing that

$$\sigma_{2x}(x) = \frac{\phi(x)}{x \tan\alpha}, \quad \sigma_{1x}(x) = \frac{p_0 - \phi(x)}{h_1 - x \tan\alpha} \quad (25)$$

from (22), (24) and (25) we find

$$\frac{d^2\phi}{dx^2} - f(x)\phi(x) = g(x)$$

$$f(x) = \frac{1}{c} \left[\frac{1-\nu_2\nu_2z}{E_{2x}x\tan\alpha} + \frac{1-\nu_1^2}{E_1(h_1-x\tan\alpha)} \right] \quad (26)$$

$$g(x) = - \frac{(1-\nu_1^2)p_0}{cE_1(h_1-x\tan\alpha)}$$

$$c = \frac{h_3\cos\alpha}{1+\tan^2\alpha} \left(\frac{1}{G_3} + \frac{\tan^2\alpha}{E_3} \right)$$

Equation (22) is solved subject to the following boundary conditions

$$\phi(0) = 0, \phi(l) = p_0 \quad (27)$$

From (25) we observe that at $x = 0$ σ_{2x} and (if $h_1 = h_2 = l\tan\alpha$) at $x = l$ σ_{1x} are not defined which may be expressed as

$$\sigma_{2x}(0) = \frac{\phi'(0)}{\tan\alpha}, \sigma_{1x}(l) = \frac{\phi'(l)}{\tan\alpha}$$

6. EXAMPLES

In the solution of the problems shown in Figures 1, 2 and 3 it will be assumed that the material 1 is aluminum, the material 2 is boron-epoxy composite and material 3 (the adhesive) is epoxy. The following elastic constants will be

used* :

Aluminum: $E_1 = 10^7$ psi, $\nu_1 = 0.3$

Boron-Epoxy: $E_{2x} = 32.4 \times 10^6$ psi, $\nu_{2x} = 0.23$,

$E_{2z} = E_{2\theta} = 3.5 \times 10^6$ psi,

$\nu_{2z} = \nu_{2\theta} = 0.03$, ($G_2 = 1.23 \times 10^6$ psi)

Epoxy: $G_3 = 1.65 \times 10^5$ psi, $E_3 = 4.45 \times 10^5$ psi

a) Bonded Plates

The following data were used in the solution of the plate problem:

$h_3 = 0.001$ in., (0.00075 in.)

$L = \ell_j - \ell_{j-1} = 0.3, 0.4, 0.5$ in., ($j = 1, \dots, 5$)

$n = 5, \ell_0 = 0$

i	1	2	3	4	5	6
h_{1i} (in.)	0.03	0.0245	0.0190	0.0135	0.008	0
h_{2i} (in.)	0.0055	0.0110	0.0165	0.0220	0.0275	0.033

* The materials and dimensions used in this study correspond to that used by W. Illg in his experimental work at NASA, Langley.

b) Reinforced Tube

The configuration of the reinforced tube is shown in Figure 2. Here the tapered portion of the aluminum tube is represented by two steps. The dimensions used in the solution of the problem are given below:

$$h_3 = 0.001 \text{ in.}, n = 6, \text{ and}$$

j	ℓ_j (in.)	r_{1j}^0 (in.)	r_{1j}^i (in.)	r_{2j}^0 (in.)	r_{2j}^i
1	0.5	.7445	.567	.750	.7445
2	1.0	.7390	.567	.750	.7390
3	1.5	.7335	.567	.750	.7335
4a	2.1	.7280	.567	.750	.728
4b	(2.0)	(.7280)	(.567)	(.750)	(.728)
5a	2.35	.728	.677	.750	.728
5b	(2.25)	(.7280)	(.642)	(.750)	(.728)
6	3.0	.728	.706	.750	.728

The dimensions in parentheses in the table above refer to an alternate representation of the tapered section of the aluminum tube. The areas S_{ij} and the thicknesses h_{ij} , used in the analysis are calculated from $S_{1j} = \pi[(r_{1j}^0)^2 - (r_{1j}^i)^2]$, $S_{2j} = \pi[(r_{2j}^0)^2 - (r_{2j}^i)^2]$, $h_{1j} = r_{1j}^0 - r_{1j}^i$, and $h_{2j} = r_{2j}^0 - r_{2j}^i$.

7. THE RESULTS AND DISCUSSION

The results for the bonded plates, in which the loads K_j at the step ends are ignored, are shown in Figures 4-11. The results are obtained for the external tensile load $p_0 = 1$, hence they have to be multiplied by the given value of p_0 (the load per unit width). Each figure contains four plots which are a) the shear stress $\tau_j(x)$ acting on the adhesive, b) total load $p_{2j}(x)$ acting on the boron-epoxy composite, c) the tensile stress σ_{2x} in boron-epoxy composite, and d) the tensile stress in aluminum.

The plate results were obtained for three values of step length ($L = 0.5, 0.4, 0.3$ in.) and for the cases $\bar{\epsilon}_z = 0$ and $\bar{\sigma}_z = 0$. The figures indicate that the difference between the two extreme assumptions regarding the boundary conditions in z direction, namely $\bar{\epsilon}_z = 0$, the fully-constrained case and $\bar{\sigma}_z = 0$, the free boundaries, is not significant. The figures also show that for the three values of L considered in this paper, the variation in the results are again negligible. In Figures 4-9, the thickness of the adhesive was assumed to be $h_3 = 0.001$ in. In Figures 10 and 11, we have $h_3 = 0.00075$ in. Comparison of the results shown in Figures 4 and 5 with that of Figures 10 and 11 show that the difference in the stresses and the load p_{2j} caused by this change in the adhesive thickness is not very significant.

In general, the figures show that in the plates bonded through a stepped joint

a) The adhesive shear stress is concentrated around the step ends $x = \ell_j$ ($j = 0, 1, \dots, n$), its maximum is at $x = 0$ and its next highest peak is at $x = \ell_n$ which is approximately 1/3 of the maximum,

b) The load $p_{2j}(x)$ varies between 0 and p_0 in a stepped fashion and the height of steps decreases as x increases,

c) The peak stress in boron-epoxy composite is at $x = \ell_1$ (at the end of the first step) which is approximately equal to $2.8 p_0/h_2$, h_2 being the full thickness of the boron-epoxy plate and,

d) The peak stress in the aluminum plate is at $x = 0$ which is equal to $(\frac{h_1}{h_{11}})/(\frac{p_0}{h_1}) = 1.18 p_0/h_1$, h_1 being the full thickness of the aluminum plate.

Table I shows a summary of some of the significant results for the bonded plates. The results given in the table were obtained from $h_3 = 0.001$ in. except for the first two rows, in which $h_3 = 0.00075$ in. was used. Note that when the thickness h_3 of the adhesive is reduced, there is some increase in the peak values of the shear stress $\tau(x)$, whereas the other quantities of interest remain basically unchanged. In the table, in all but the last two rows, it was assumed that $K_j = 0$, ($j = 0, 1, \dots, n$). The last two rows will be dis-

TABLE I

Summary of the Plate Results ($h_3 = 0.001$ in.)

L (in.)	$\bar{\epsilon}_z, \bar{\sigma}_z$	$\frac{p_{2\max}}{p_0}$ ($x = l_n$)	$\frac{\tau_{\max}}{(p_0/h_2)}$ ($x = 0$)	$\frac{\sigma_{1\max}}{(p_0/h_1)}$ ($x = 0$)	$\frac{\sigma_{2\max}}{(p_0/h_2)}$ ($x = l_1$)
0.5 ($h_3 = 0.00075$)	$\bar{\epsilon}_z = 0$	1.0	0.506	1.18	2.72
($K_j = 0$)	$\bar{\sigma}_z = 0$	1.0	0.543	1.18	2.85
0.5	$\bar{\epsilon}_z = 0$	1.0	0.440	1.18	2.72
($K_j = 0$)	$\bar{\sigma}_z = 0$	1.0	0.470	1.18	2.85
0.4	$\bar{\epsilon}_z = 0$	1.0	0.439	1.18	2.72
($K_j = 0$)	$\bar{\sigma}_z = 0$	1.0	0.470	1.18	2.85
0.3	$\bar{\epsilon}_z = 0$	1.0	0.438	1.18	2.72
($K_j = 0$)	$\bar{\sigma}_z = 0$	1.0	0.470	1.18	2.85
0.3 ($d_3 = 0.01$)	$\bar{\sigma}_z = 0$	0.994	0.441	1.16	2.87
0.3 ($d_3 = 0.001$)	$\bar{\sigma}_z = 0$	0.964	0.285	1.01	3.12

cussed later in the paper.

The results for the reinforced tube are shown in Figures 12 and 13. The difference between the two figures is in the representation of the tapered part of the aluminum tube by different steps (see Figure 2). The quantities which seem to be more sensitive to this difference are the adhesive shear stress $\tau(x)$ and the tensile stress in the aluminum tube which have sharp peaks at the locations of assumed discontinuity. In the actual case, in which there is no discontinuity in the tube thickness, the shear stress and the stress in the aluminum tube are likely to be of the form shown by dashed lines in Figure 12a and Figure 12d.

In this problem the maximum shear acting on the adhesive is also at $x = 0$. The stress in boron-epoxy composite has its maximum at $x = \ell_n$, (that is, the mid-plane) where approximately 77% of the total load p_0 is carried by this material. The peak stress in aluminum tube is around $x = \ell_{n-1}$, which is roughly the end of the tapered section.

To study the effect of the bonding loads K_j , ($j = 0, \dots, n$) at the step ends, the problem described in Section 4 was solved for the plates with $L = 0.3$ in., $h_3 = 0.001$ in., $\bar{\sigma}_z = 0$, $p_0 = 1$ and for two values of d_3 , $d_3 = 0.01$ in. and $d_3 = 0.001$ in. The results are shown in Figures 14 and 15. The values of the end loads K_j were found to be as follows:

d_3	K_0	K_1	K_2	K_3	K_4	K_5
0.01	0.0226	-0.00684	-0.00425	-0.00319	-0.00279	0.00599
0.001	0.1462	-0.0949	-0.0577	-0.0443	-0.0414	0.0363

It is seen that at the two extreme ends K_0 and K_5 are tensile and the remaining K_j 's are compressive. Also, by decreasing d_3 by one order of magnitude, it is seen that K_j 's are increased also by approximately one order of magnitude. Comparison of Figures 9 and 14 shows that for $d_3 = 0.01$ the solutions obtained by assuming $K_j = 0$ and $K_j \neq 0$ are roughly the same. On the other hand, as d_3 decreases the differences in the calculated stresses may be significant. This can also be seen from Table I by comparing the values given in the last three rows where the last two rows show the results of the analysis with $K_j \neq 0$. For the smaller value of d_3 , even though there is a slight increase in the stress concentration factor in boron-epoxy plate, there is also a significant decrease in τ_{max} . In this example d_3 was assumed to have the same value at all step ends. However, the analysis is general and d_3 may have different values at different step ends. It is clear that the ends with smaller adhesive thickness d_3 would carry larger loads.

Finally, Figures 16 and 17 show the results for aluminum and boron-epoxy plates bonded through a smoothly tapered joint

shown in Figure 3. Here (26) is solved with

$$h_3 = 0.001 \text{ in.}, \tan \alpha = \frac{0.0055}{L}, L = 0.3, 0.5 \text{ in.}$$

$$h_1 = h_2 = 0.033 \text{ in.}, p_0 = 1$$

It is obvious that these results have all the basic trends of the solution of the stepped joint problem, except that, as it is expected, all the quantities are smooth functions of x . The main results of this solution can be summarized as follows:

a) In the joint, the greater portion of the load is carried by the stiffer material (i.e., the boron-epoxy plate). For $0 < x < \ell$ the stress in aluminum is always less than, and the stress in boron epoxy plate is always greater than the average stress p_0/h_2 acting outside the joint. In fact for $h_1 = h_2$ we have $\sigma_{2\text{min.}} = \frac{p_0}{h_2} = \sigma_{1\text{max.}}$, σ_1 and σ_2 being the stresses in aluminum and boron-epoxy, respectively*.

* This result is consistent with that found in [2], where it is shown that in bonded isotropic wedges with $h_3 = 0$, $\nu_1 = \nu_2$ and total angle = π , if the modulus E_1 of the wedge with the smaller angle is less than E_2 , the modulus of the wedge with the greater angle, the stresses at the apex are finite, and if $E_1 > E_2$ the stresses at the apex have a singularity. In the present problem $x = \ell$ correspond to the former and $x = 0$ correspond to the latter case. Thus, it is expected that the stresses in the neighborhood of $x = 0$ would be much higher than that around $x = \ell$. As seen from Figures 16 and 17, this is clearly the case. In this problem too the consideration of the adhesive as a separate layer removes the singularity and renders the stresses finite throughout the body.

b) The contact shear stress $q(x)$ has only one peak (at $x = 0$) and is a rather smooth function of x . As a result, the maximum value of $q(x)$ is much smaller than that corresponding to the stepped joints, in which the load transfer takes place largely around the end points of the steps (see Figures 4-15). For $h_1 = h_2 = 0.033$ in., the following table shows the extreme values of the stresses*:

ℓ (in.)	$\underline{q_{max}}$	$\underline{q_{min}}$	$\underline{\sigma_{1max}}$	$\underline{\sigma_{1min}}$	$\underline{\sigma_{2max}}$	$\underline{\sigma_{2min}}$
	(p_0/h_2) ($x = 0$)	(p_0/h_2) ($x = \ell$)	(p_0/h_2) ($x = 0$)	(p_0/h_2) ($x = \ell$)	(p_0/h_2) ($x = 0$)	(p_0/h_2) ($x = \ell$)
1.8	0.053	0.00612	1.0	0.338	2.897	1.0
3.0	0.032	0.00367	1.0	0.338	2.910	1.0

Note that the stress concentration in boron-epoxy in the tapered joint is roughly the same as that in the stepped joint. However, there is an order of magnitude difference in the maximum values of the adhesive shear stress.

REFERENCES

1. F. Erdogan, "Distribution of Adhesive Shear Stress in a Stiffened Plate", Technical Progress Report to NASA, Grant No. NGR-39-007-011, December 1969.

* The normal component of the contact stress, $p(x)$ is not given in the Figures or the Table. It can simply be obtained from (21), i.e., $p(x) = q(x)\tan\alpha$.

2. V. L. Hein and F. Erdogan, "Stress Singularities in a Two-Material Wedge", to appear in the Int. J. Fracture Mechanics, 1971.

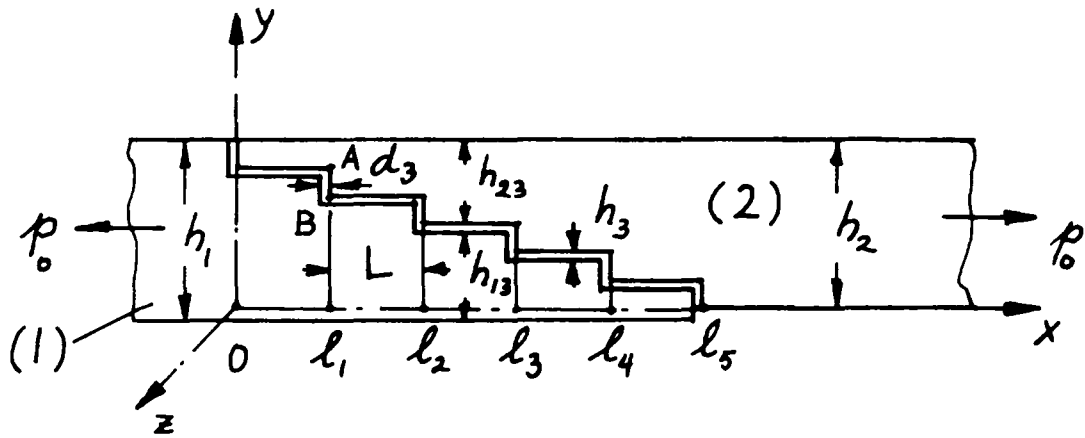


FIGURE 1. BONDED PLATES WITH A STEPPED JOINT

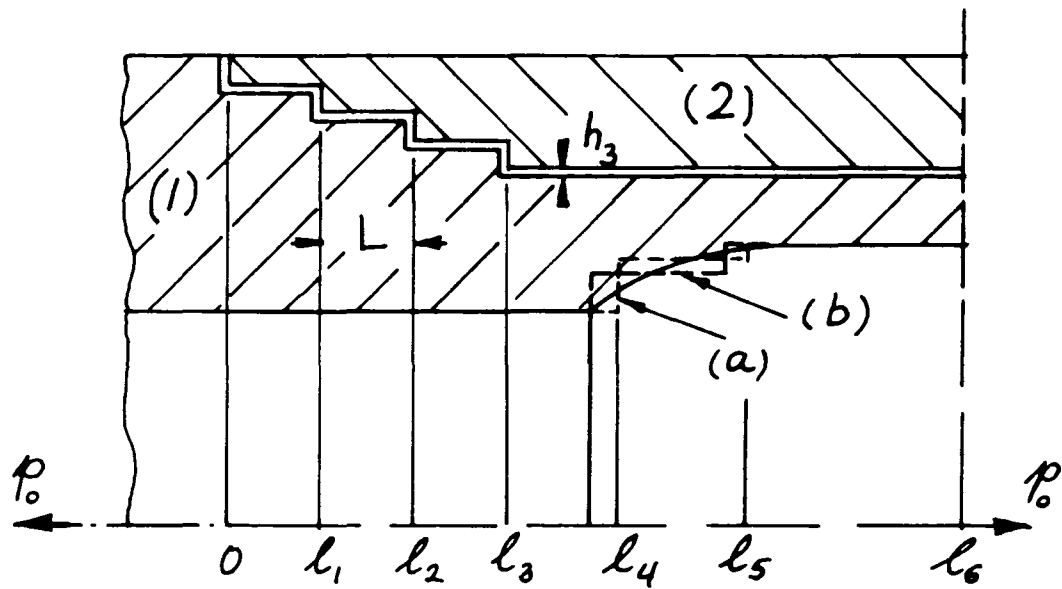


FIGURE 2. REINFORCED TUBE WITH A STEPPED JOINT

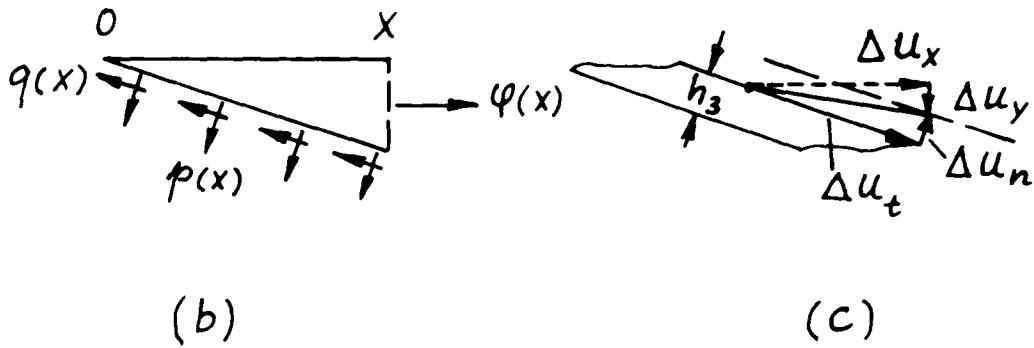
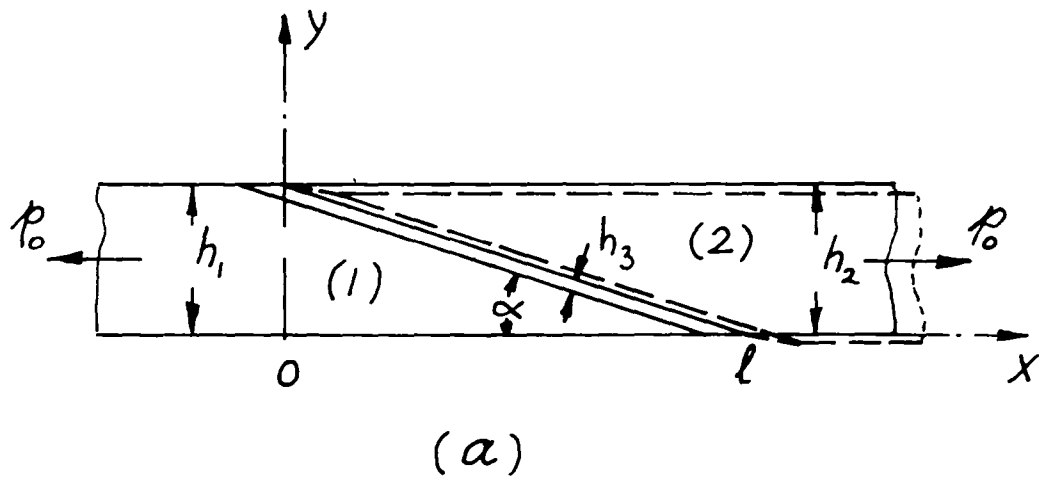


FIGURE 3. BONDED PLATES WITH A SMOOTHLY TAPERED JOINT

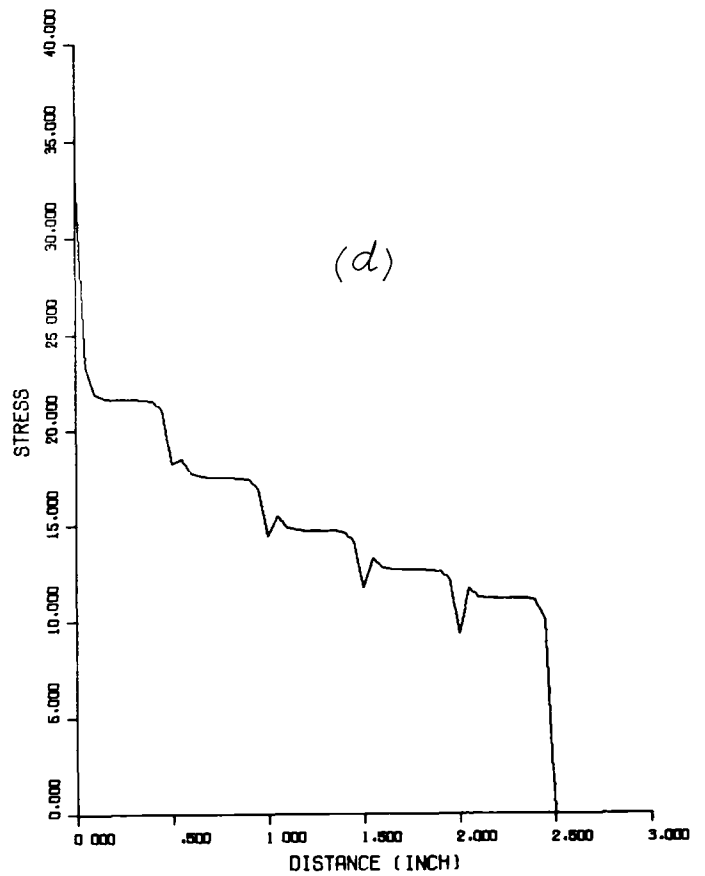
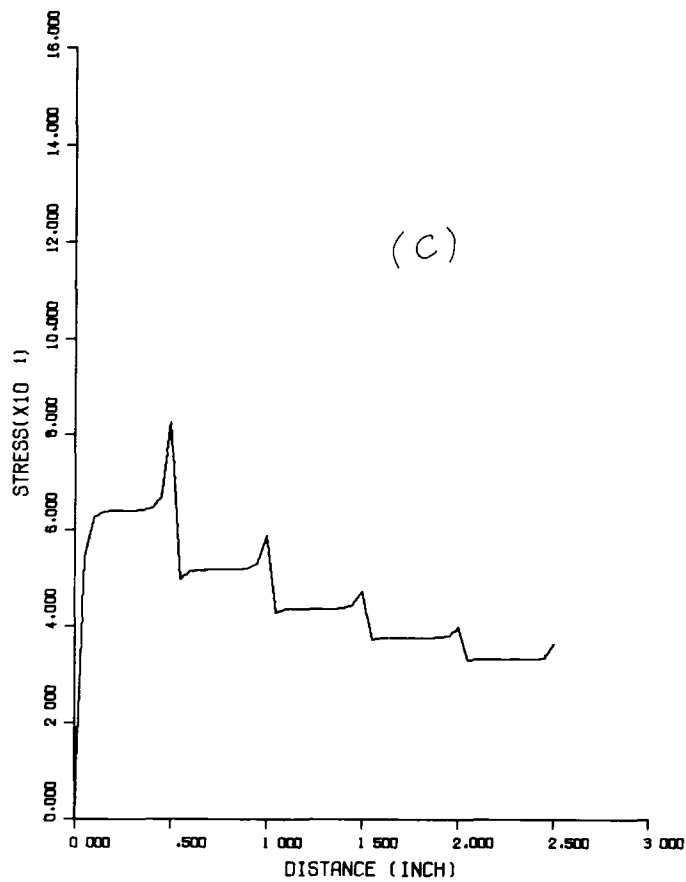
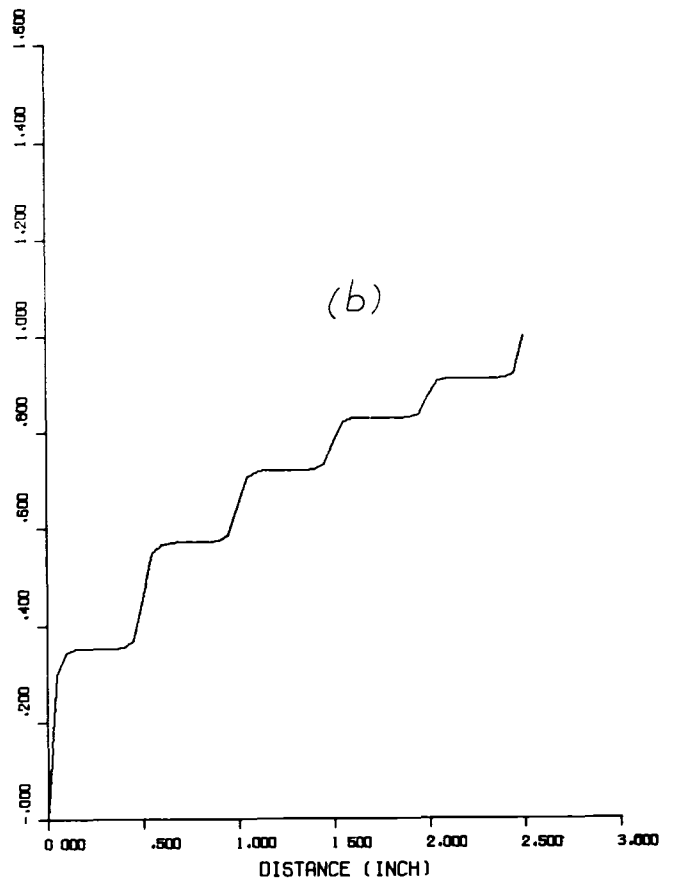
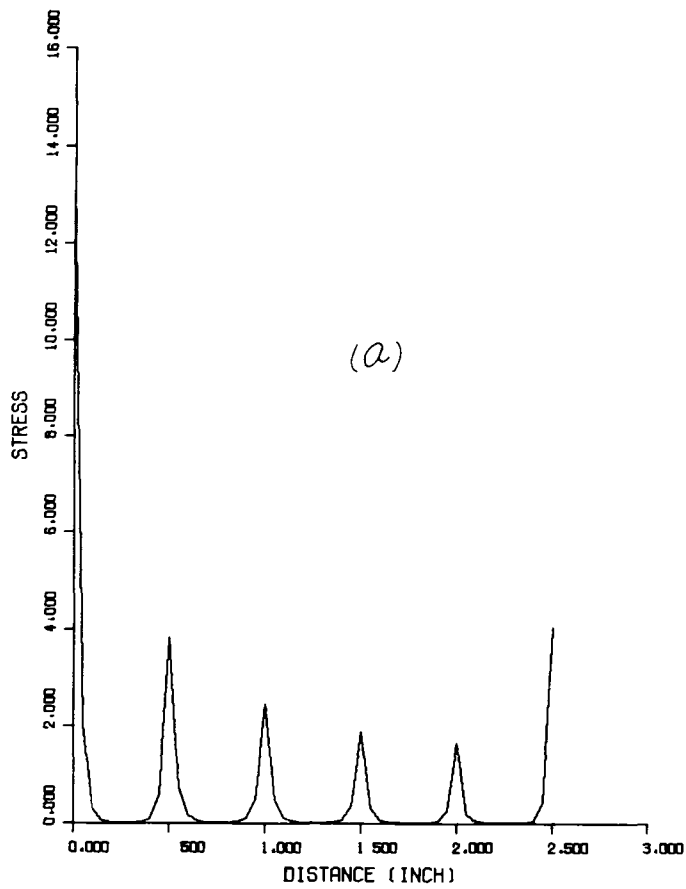


FIGURE 4 BONDED ALUMINUM-BORON EPOXY PLATES WITH $\bar{e}_z = 0$, $L = 0.5$ IN, $K_j = 0$, $h_3 = 0.001$ IN, $P_0 = 1$

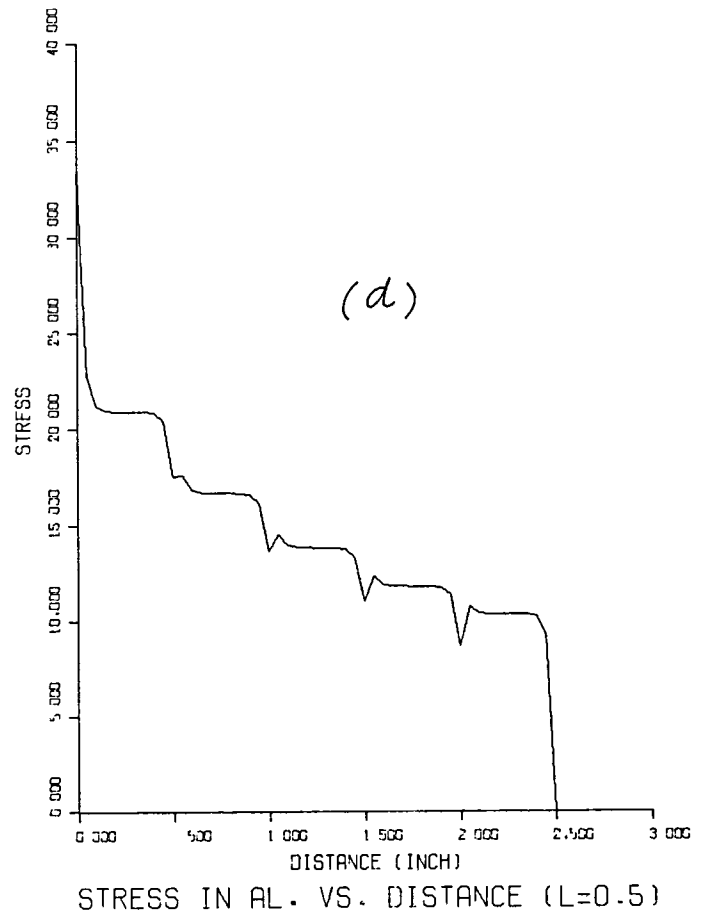
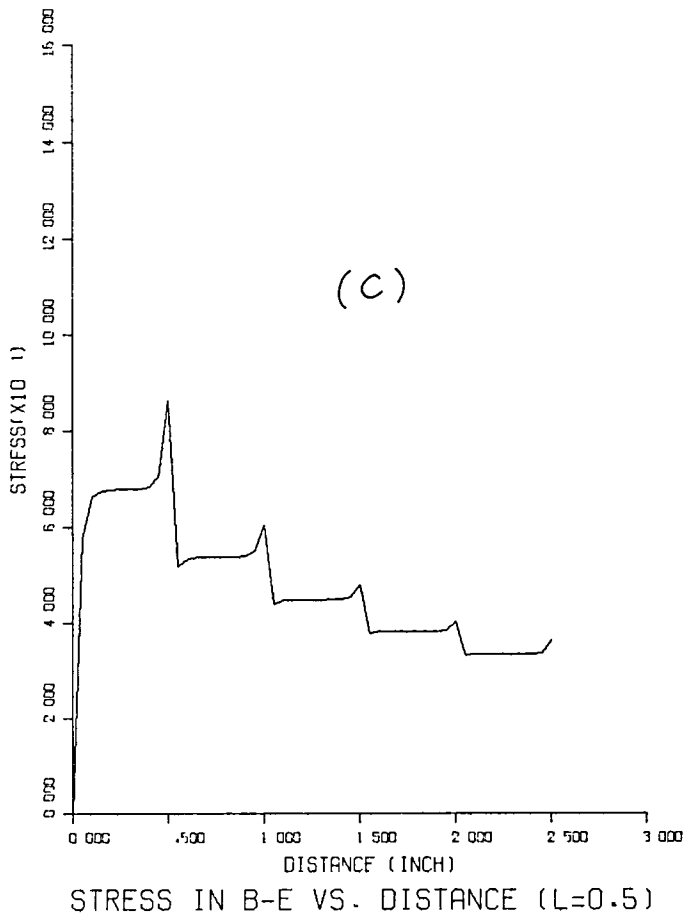
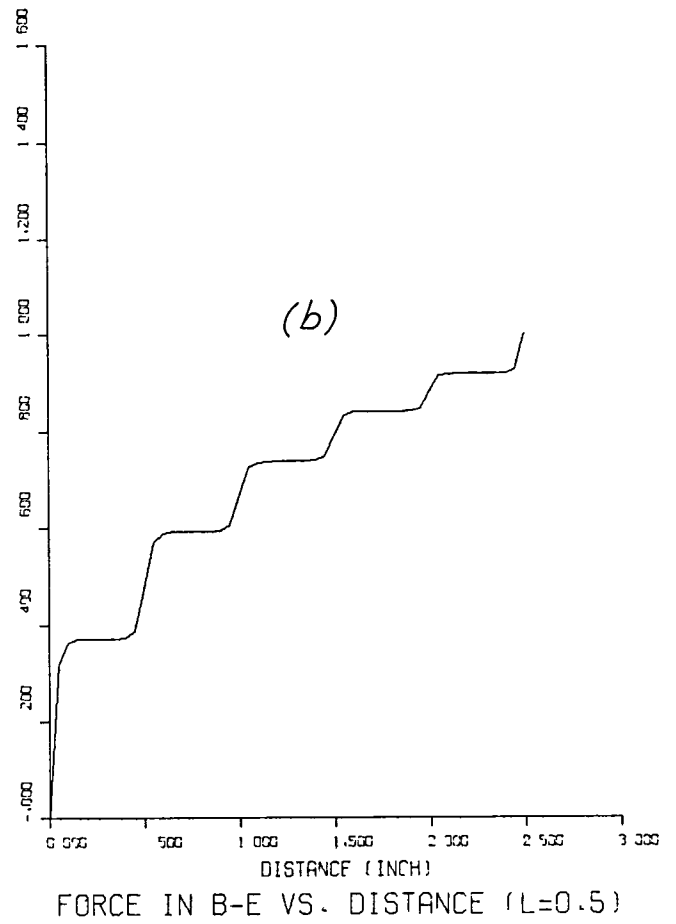
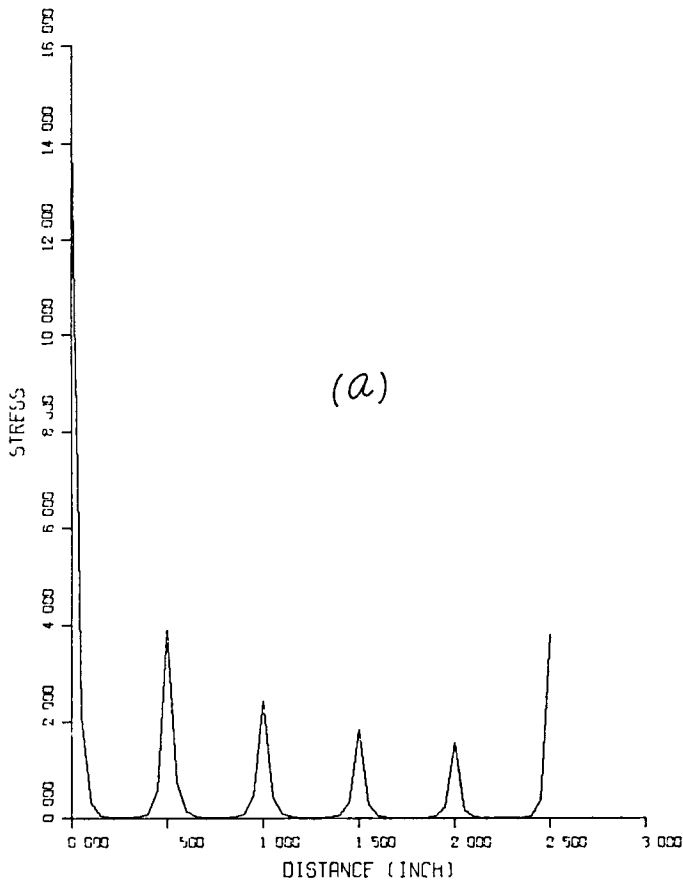
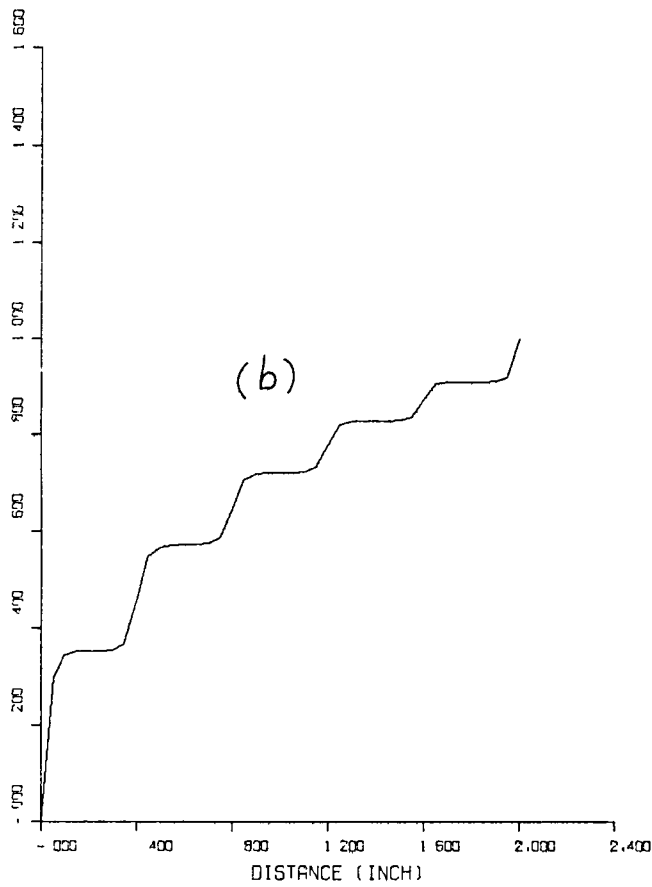
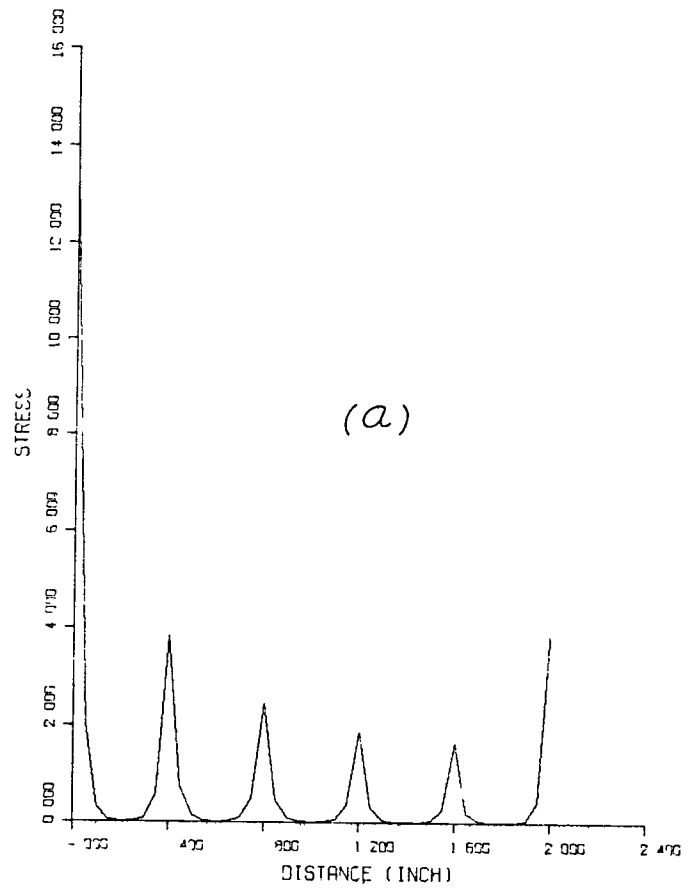


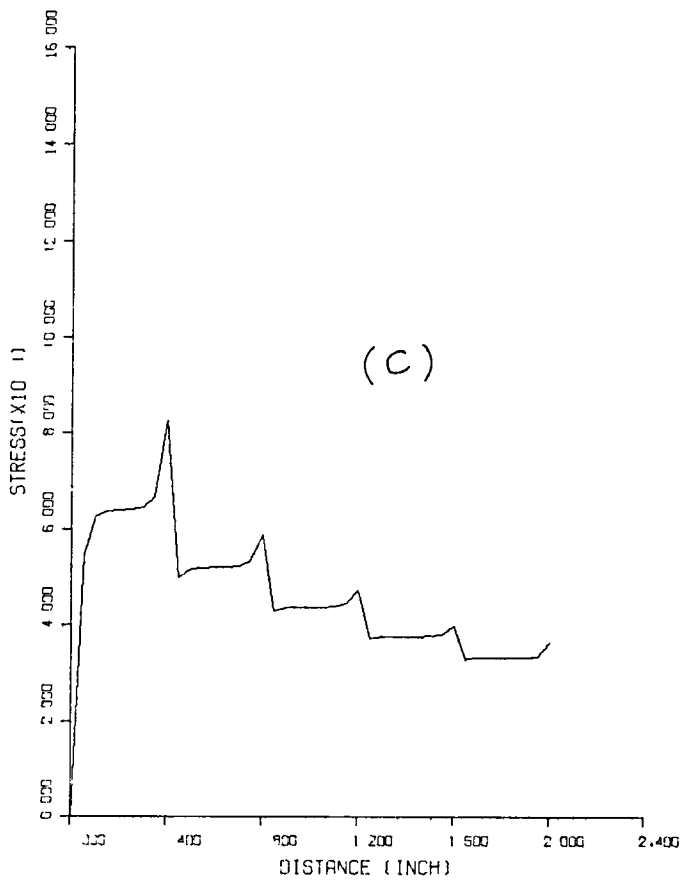
FIGURE 5 BONDED ALUMINUM-BORON EPOXY PLATES WITH $\bar{\sigma}_2 = 0$, $L = 0.5$ IN., $K_j = 0$, $h_3 = 0.001$ IN., $p_0 = 1$



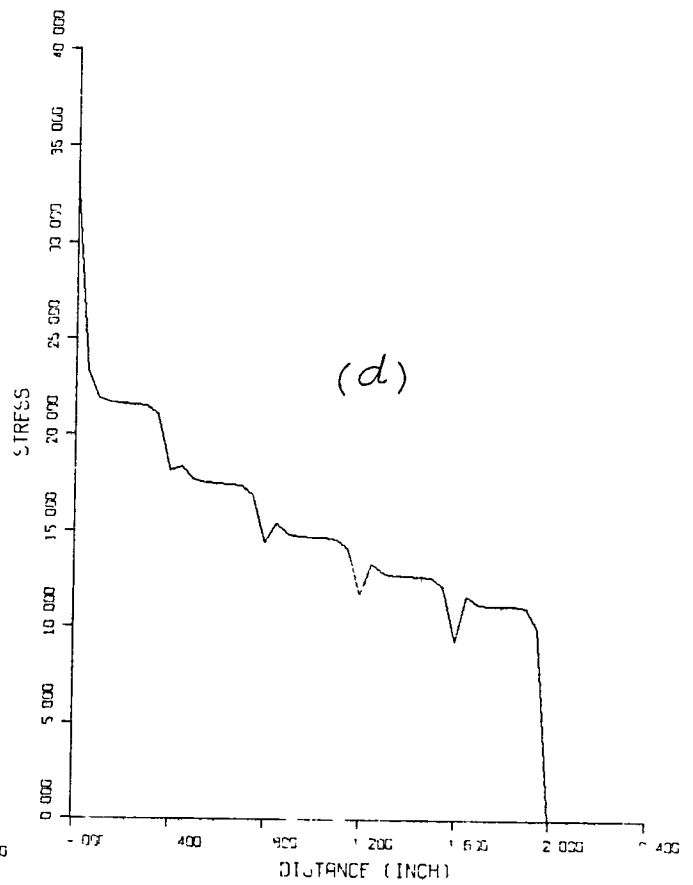
FORCE IN B-E VS. DISTANCE (L=0.4)



SHEAR STRESS VS. DISTANCE (L=0.4)

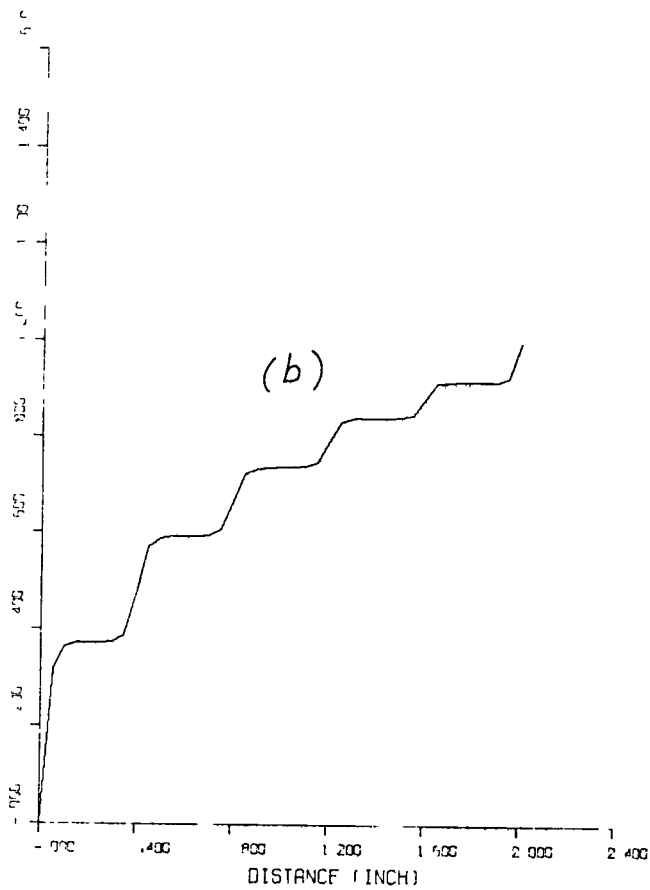


STRESS IN B-E VS. DISTANCE (L=0.4)

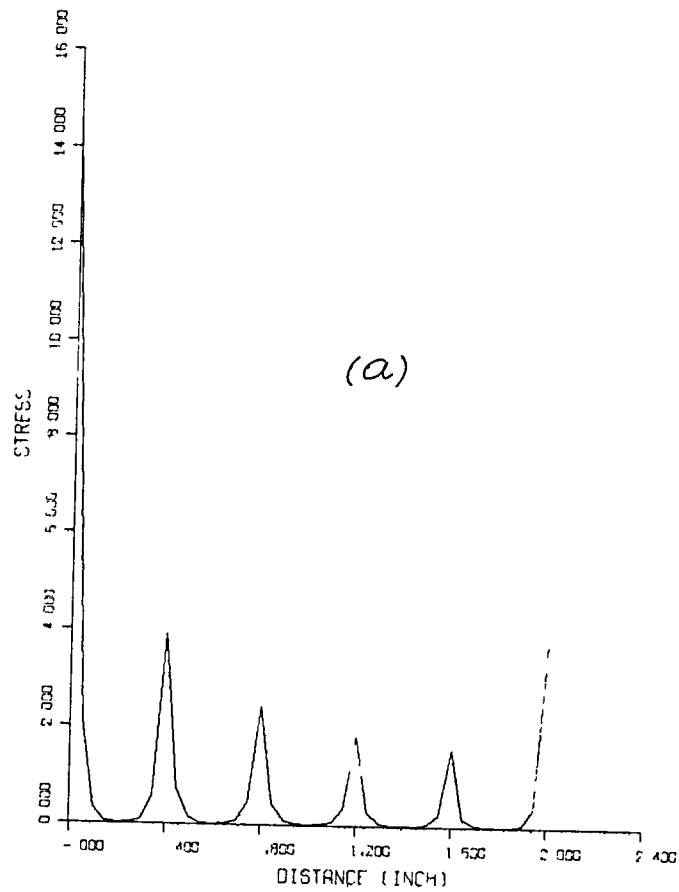


STRESS IN AL. VS. DISTANCE (L=0.4)

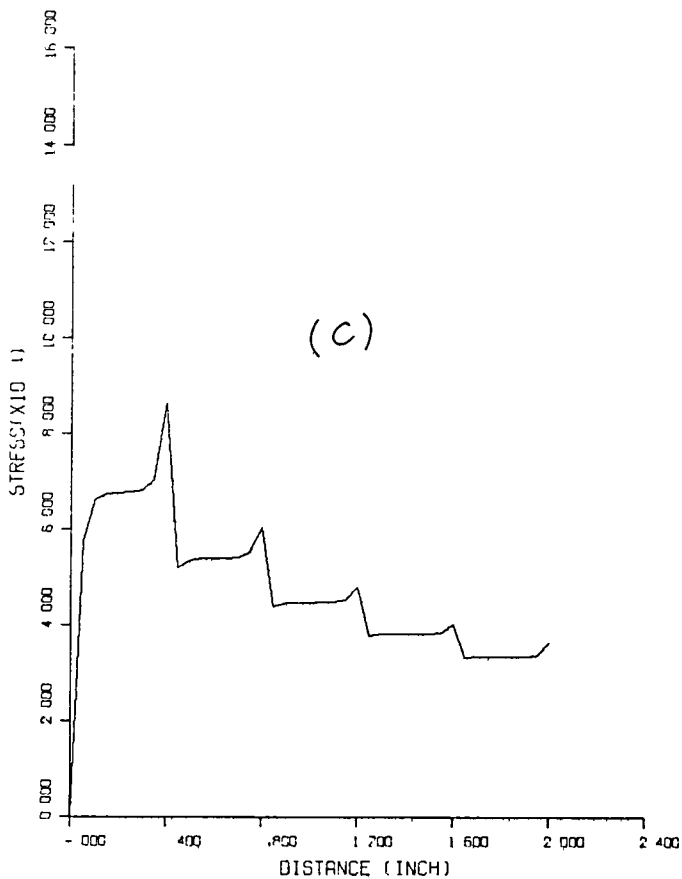
FIGURE 6 BONDED ALUMINUM-BORON EPOXY PLATES WITH $\bar{\epsilon}_z = 0$, $L = 0.4$ IN., $K_j = 0$, $h_3 = 0.001$ IN., $p_0 = 1$



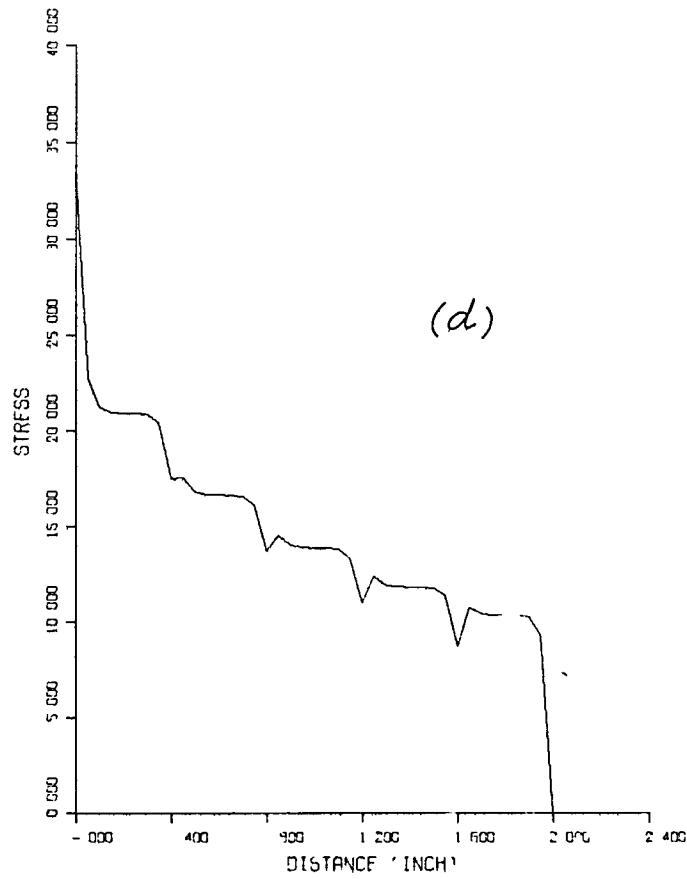
FORCE IN B-E VS. DISTANCE (L=0.4)



SHEAR STRESS VS. DISTANCE (L=0.4)

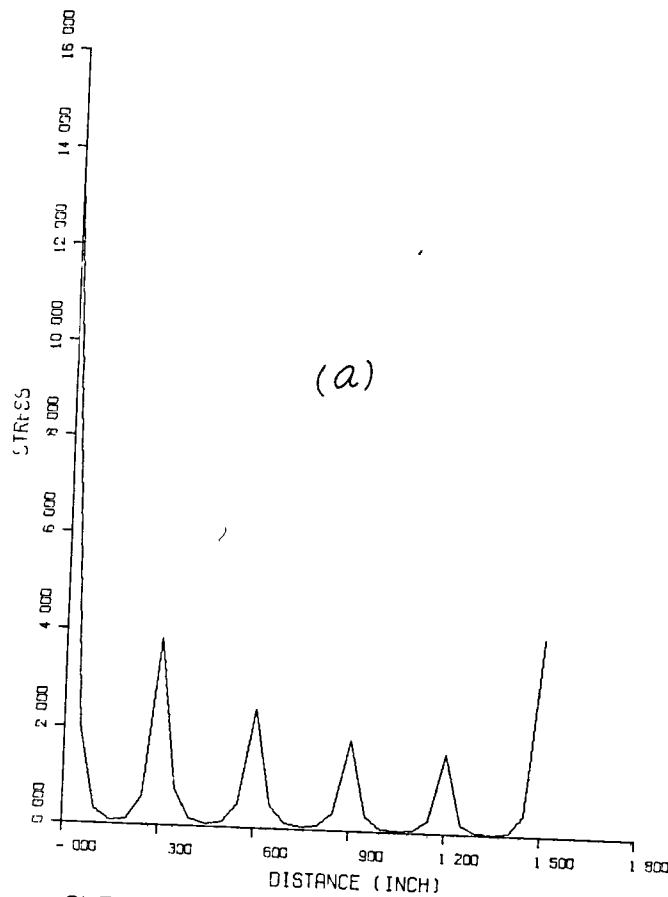


STRESS IN B-E VS. DISTANCE (L=0.4)

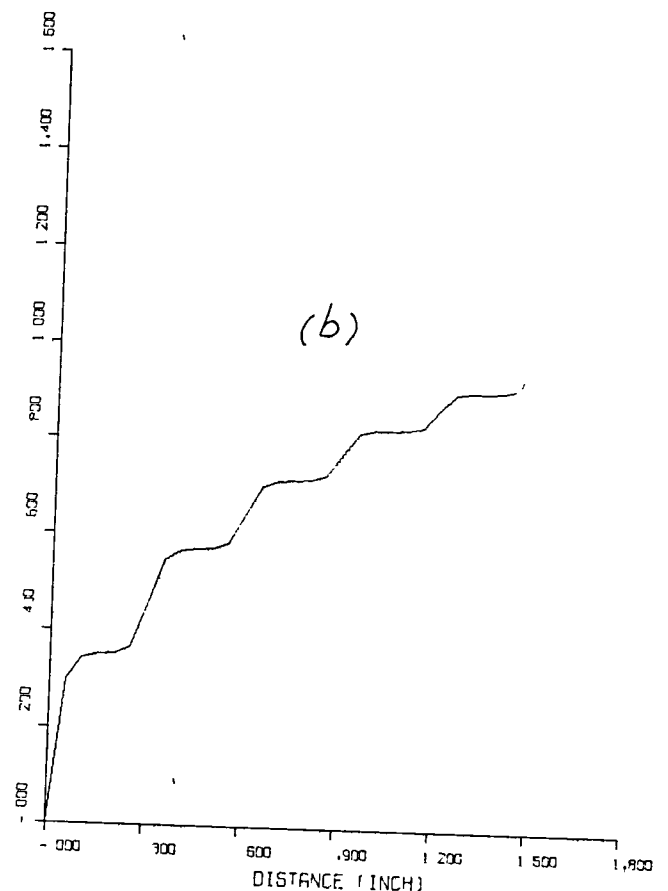


STRESS IN AL. VS. DISTANCE (L=0.4)

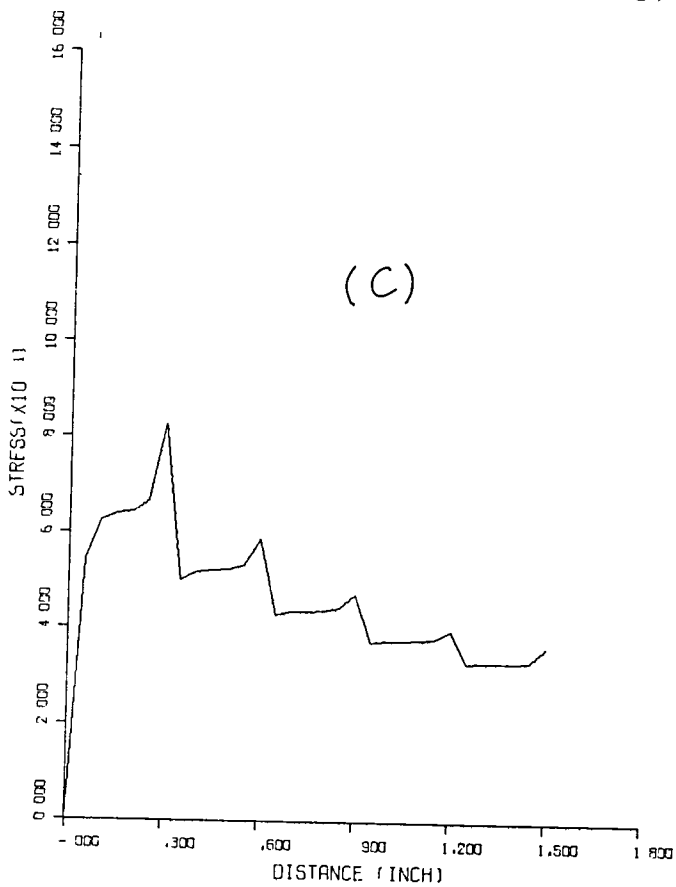
FIGURE 7 BONDED ALUMINUM-BORON EPOXY PLATES WITH $\bar{v}_z = 0$, $L = 0.4$ IN, $K_j = 0$, $h_3 = 0.001$ IN, $P_0 = 1$



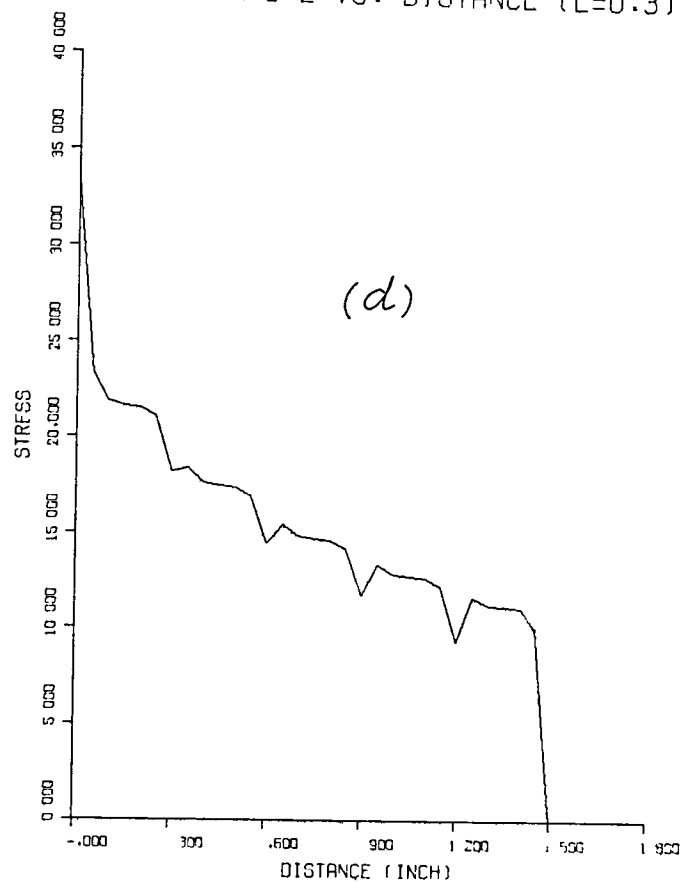
SHEAR STRESS VS. DISTANCE (L=0.3)



FORCE IN B-E VS. DISTANCE (L=0.3)

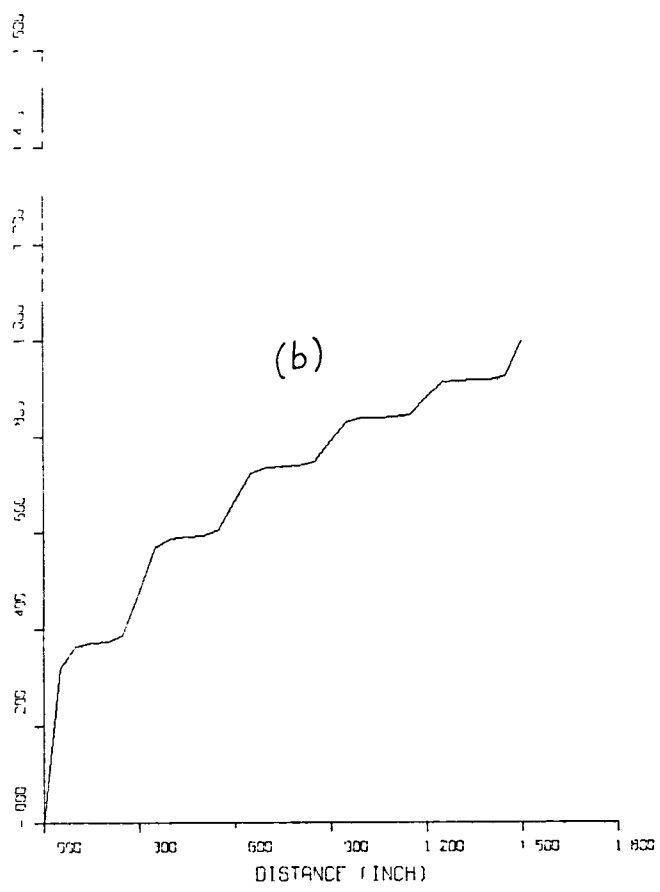


STRESS IN B-E VS. DISTANCE (L=0.3)

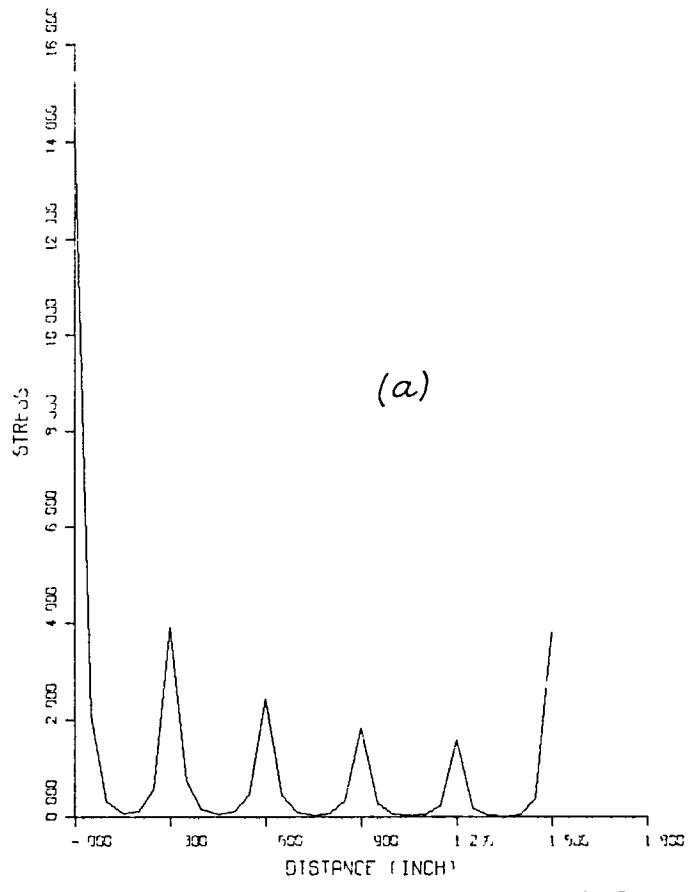


STRESS IN AL. VS. DISTANCE (L=0.3)

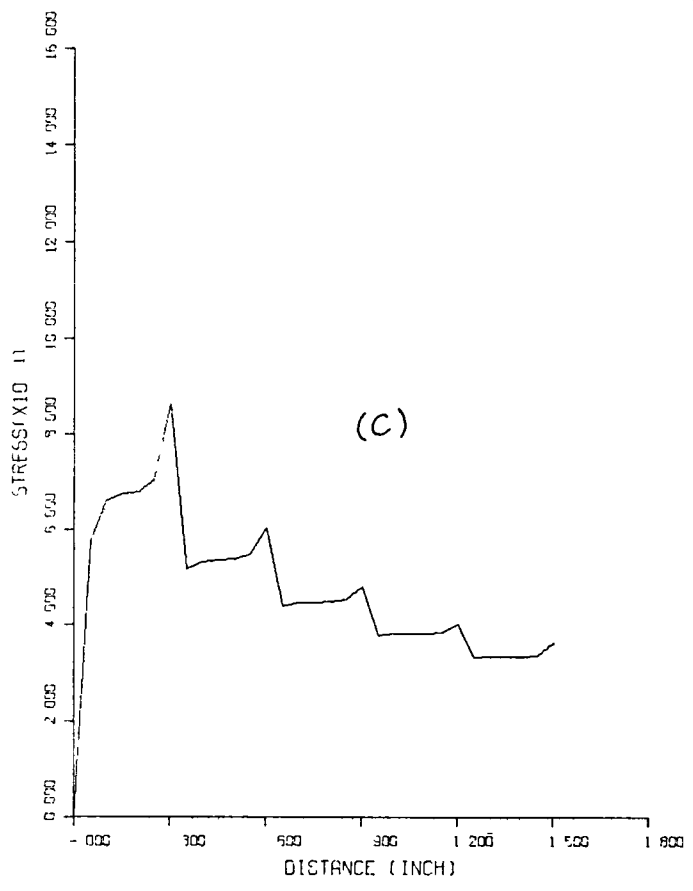
FIGURE 8 BONDED ALUMINUM-BORON EPOXY PLATES WITH $\bar{\epsilon}_2 = 0$, $L = 0.3$ IN, $K_j = 0$, $h_3 = 0.001$ IN, $p_0 = 1$



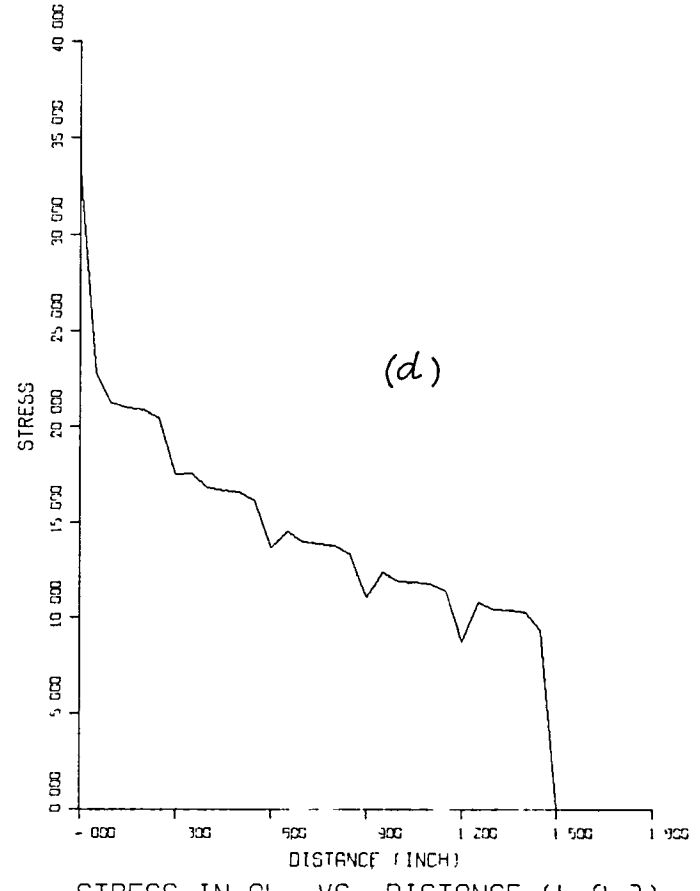
FORCE IN B-E VS. DISTANCE (L=0.3)



SHEAR STRESS VS DISTANCE (L=0.3)



STRESS IN B-E VS. DISTANCE (L=0.3)



STRESS IN AL. VS. DISTANCE (L=0.3)

FIGURE 9 BONDED ALUMINUM-BORON EPOXY PLATES WITH $\sigma_2 = 0$, $L = 0.3$ IN, $K_j = 0$, $h_3 = 0.001$ IN, $P_0 = 1$

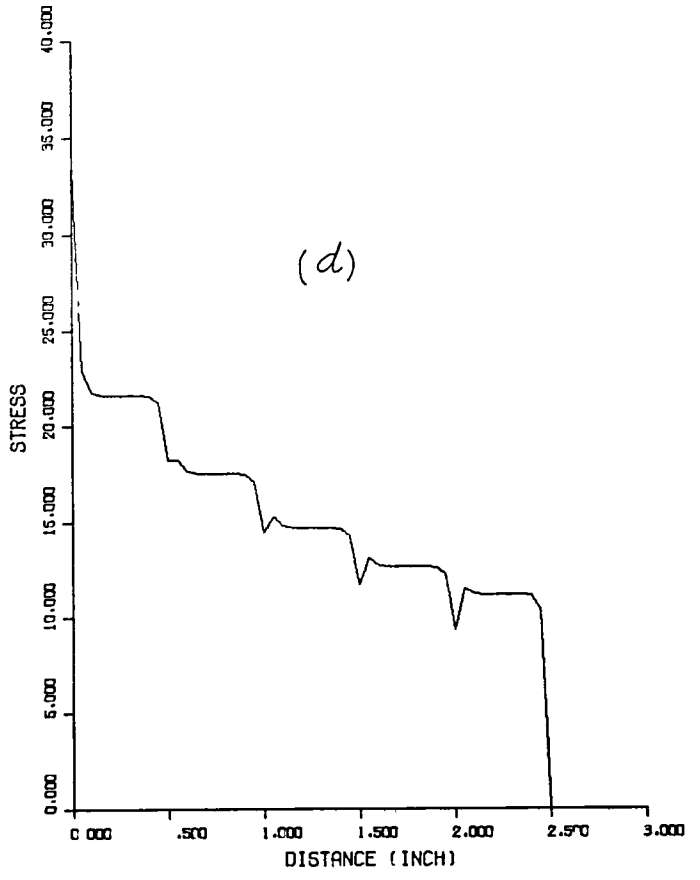
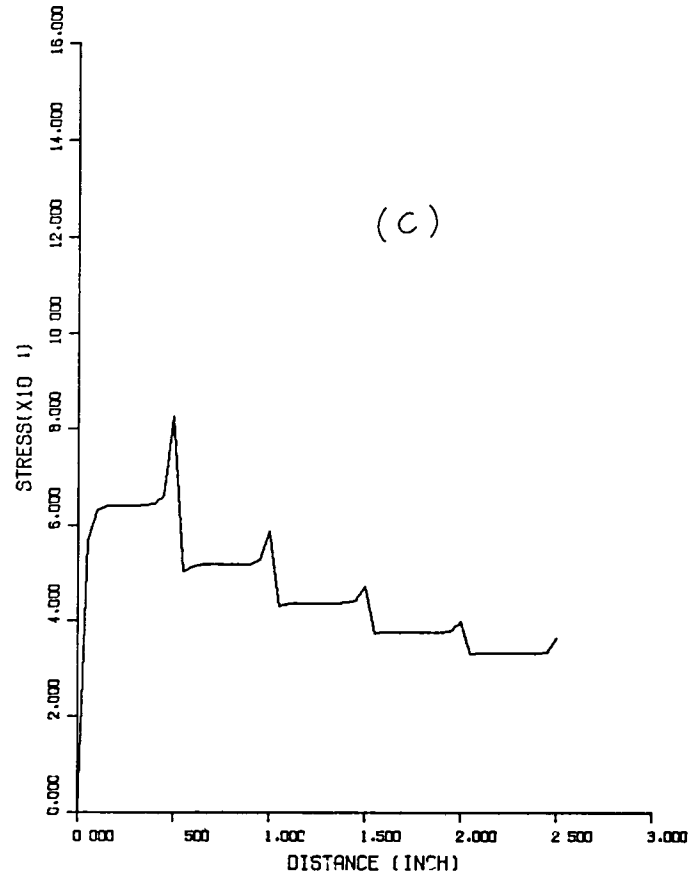
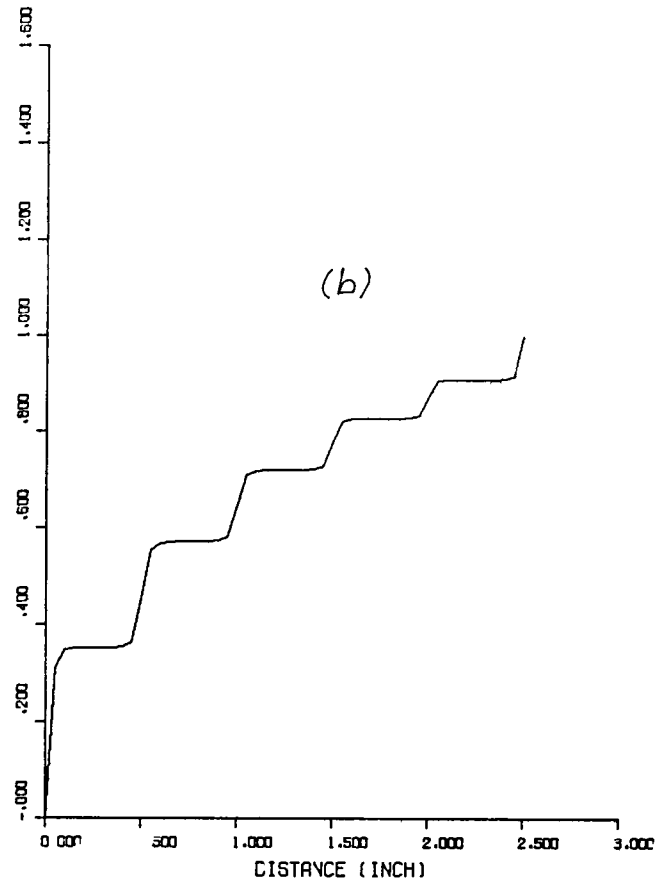
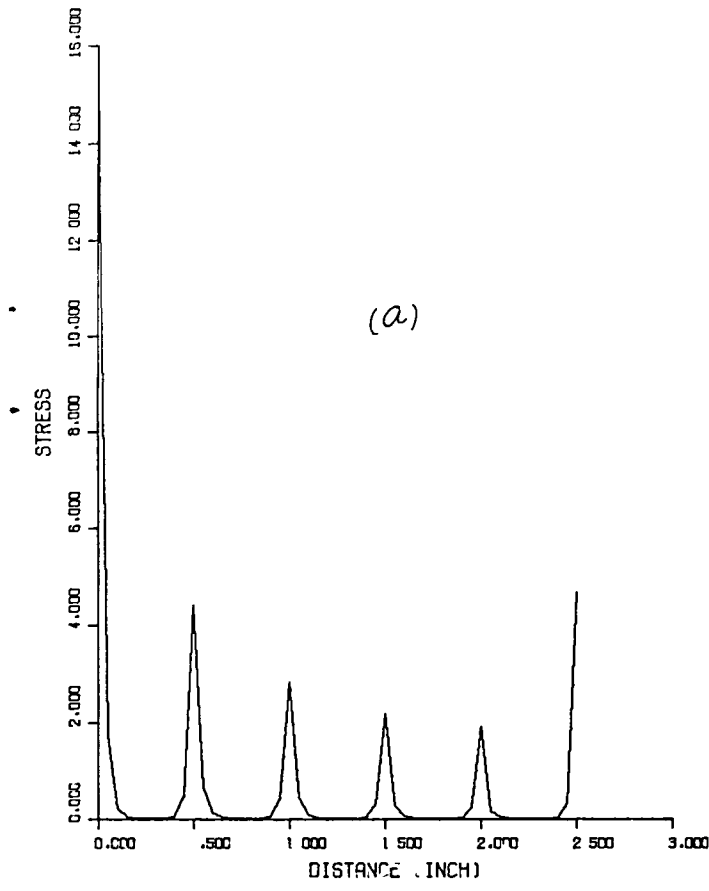


FIGURE 10 BONDED ALUMINUM-BORON EPOXY PLATES WITH $\bar{\epsilon}_2 = 0$, $L = 0.5$ IN, $K_J = 0$, $h_3 = 0.00075$ IN, $\rho_0 = 1$

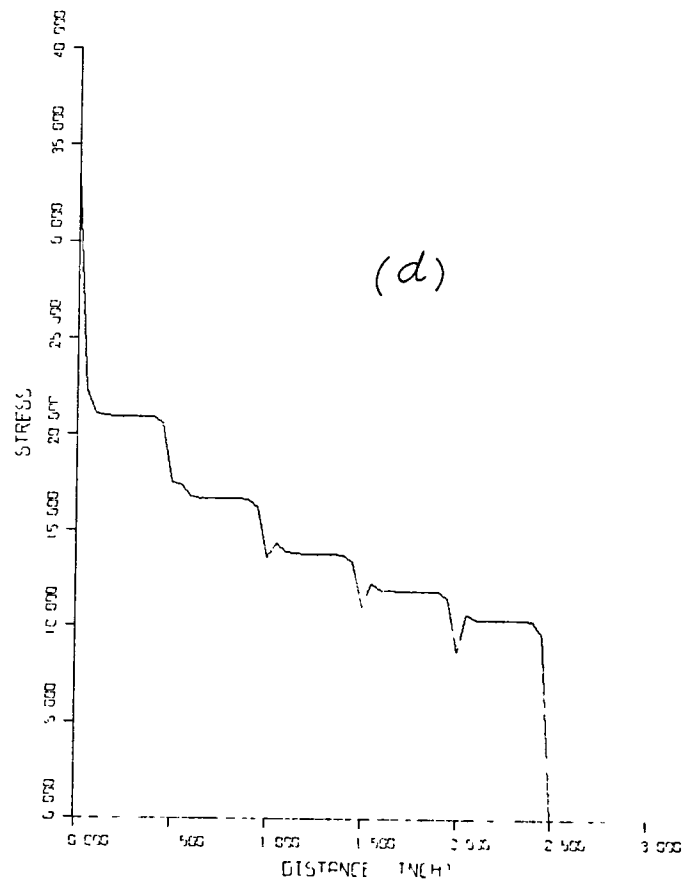
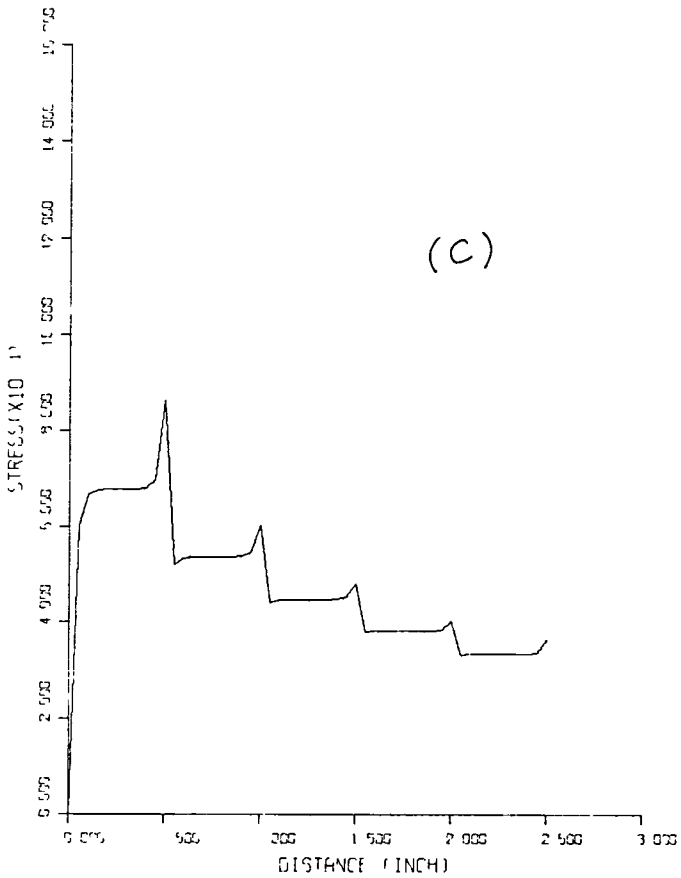
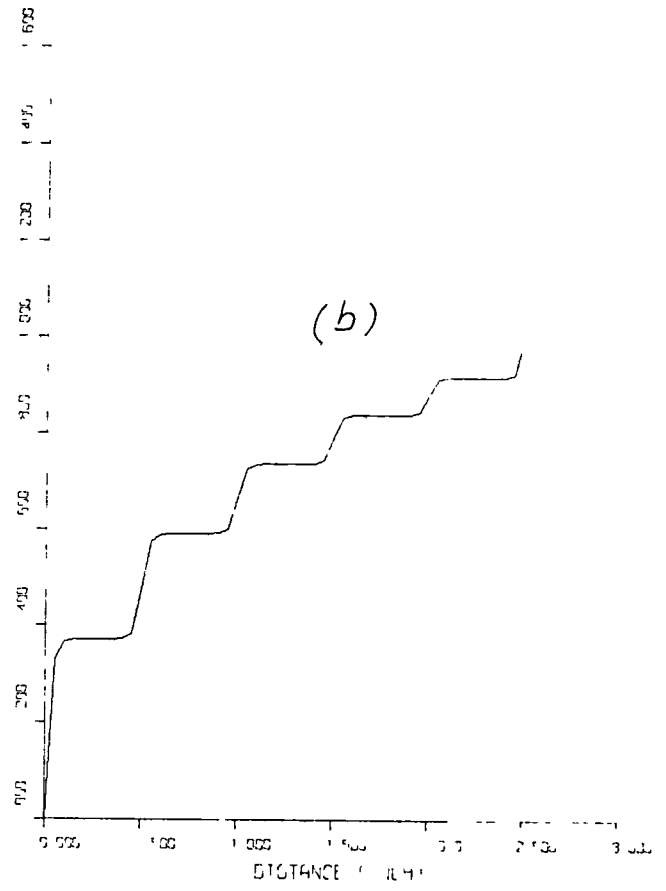
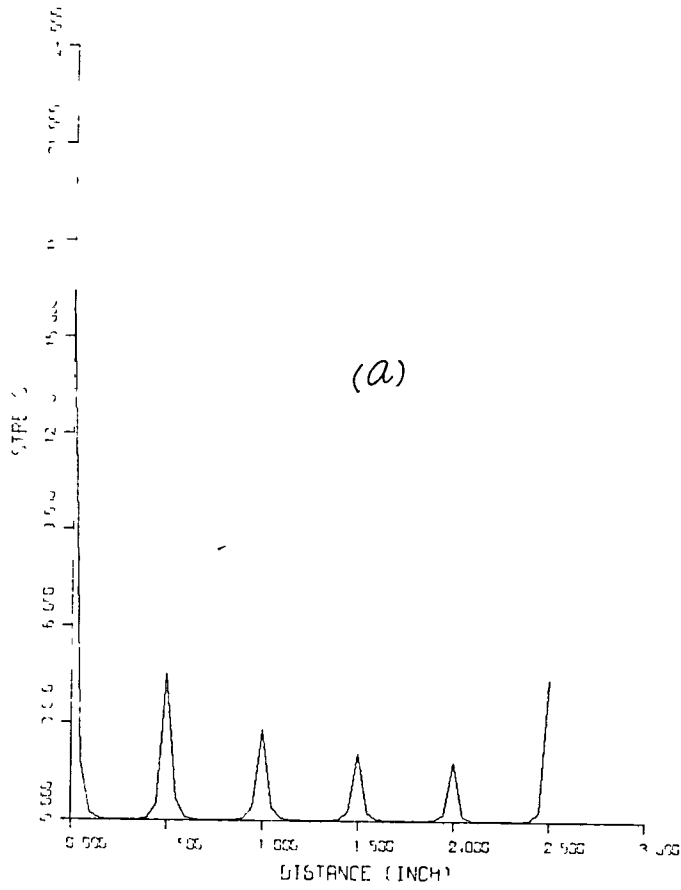
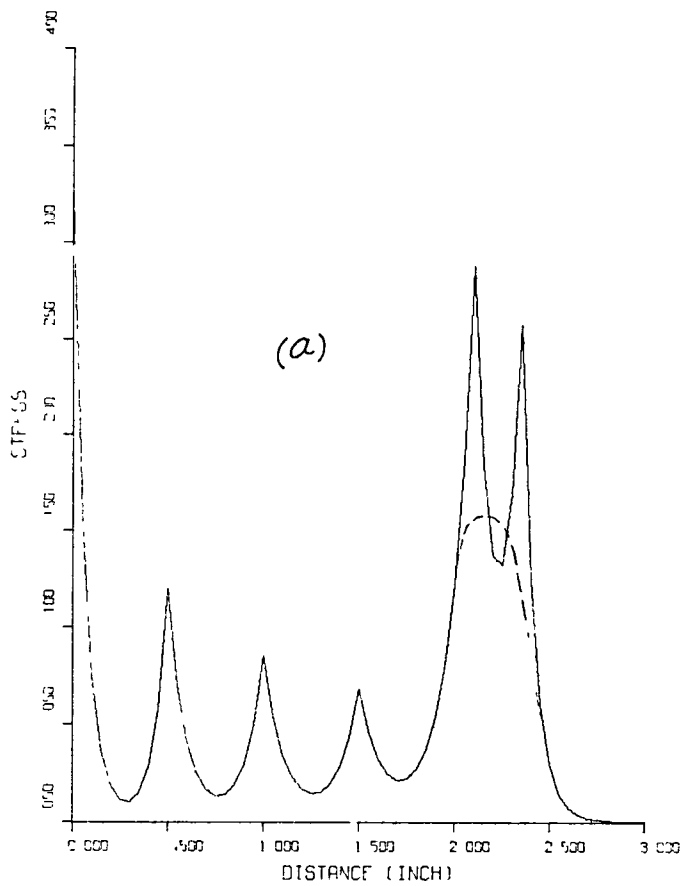
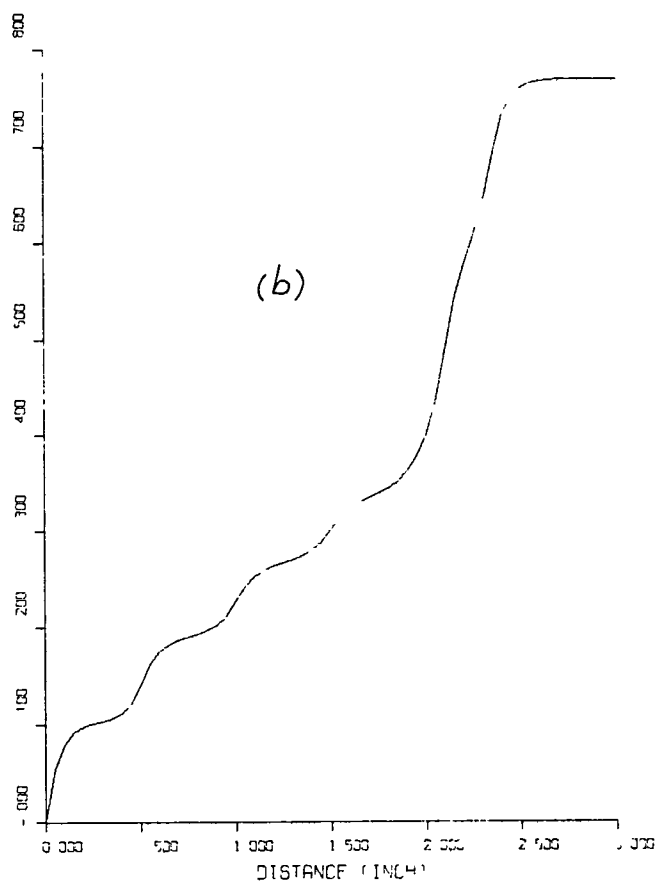


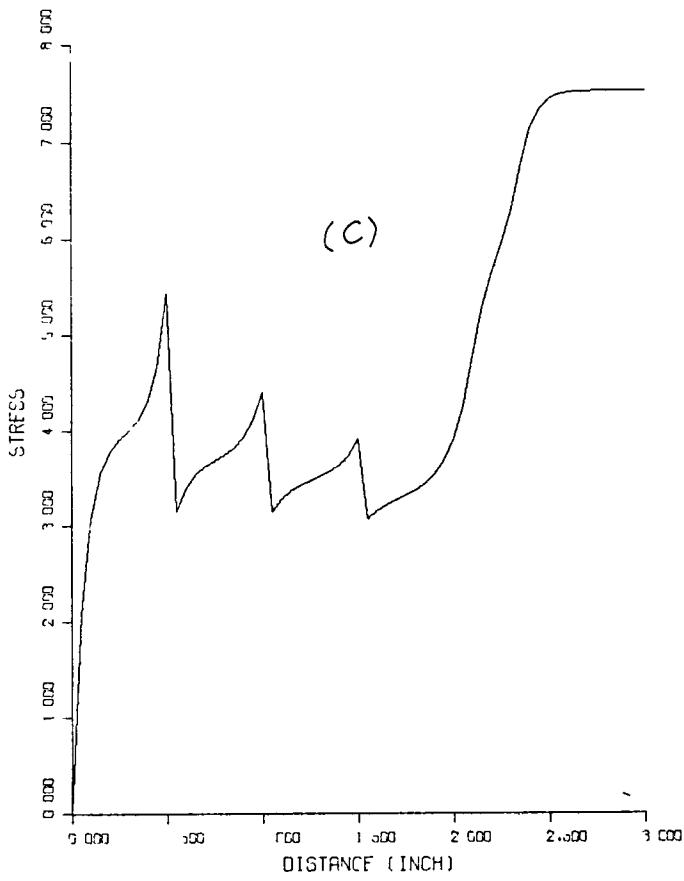
FIGURE 11 BONDED ALUMINUM-BORON EPOXY PLATES WITH $\sigma_z = 0$, $L = 0.5$ IN, $K_j = 0$, $h_3 = 0.00075$ IN, $P_0 = 1$



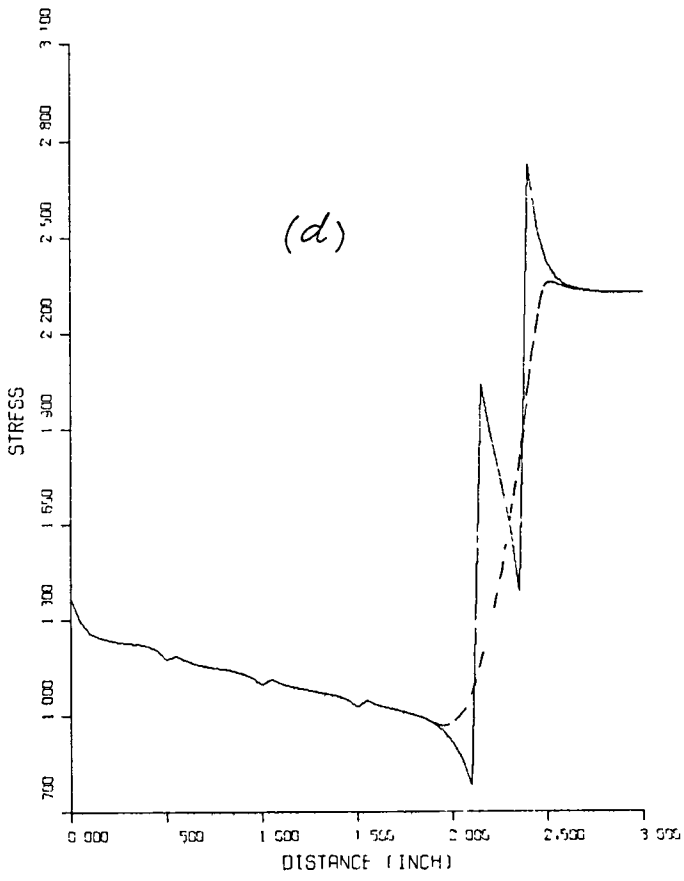
(a) SHEAR STRESS VS. DISTANCE



(b) FORCE IN B-E VS. DISTANCE

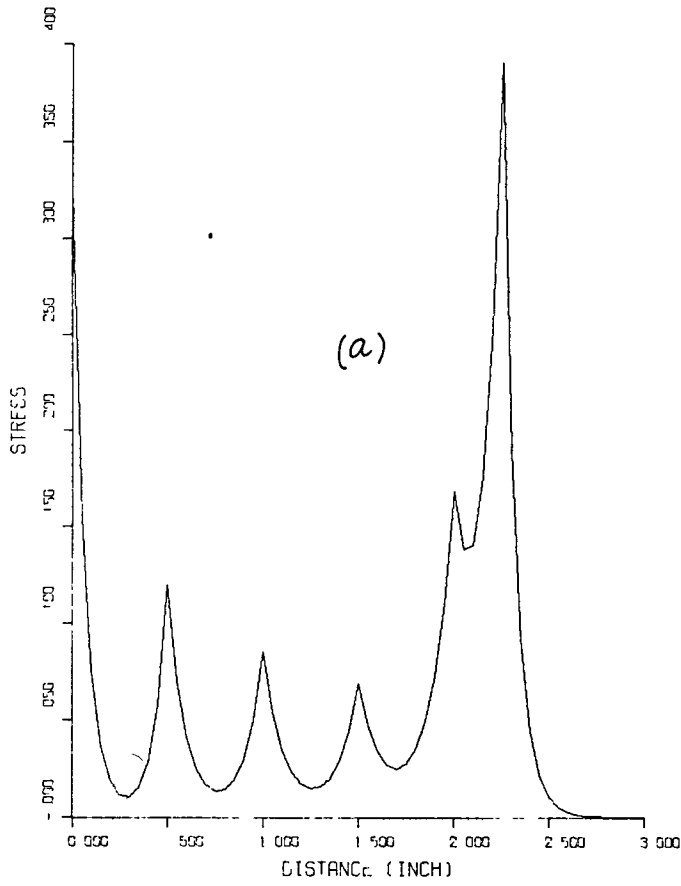


(c) STRESS IN B-E VS. DISTANCE

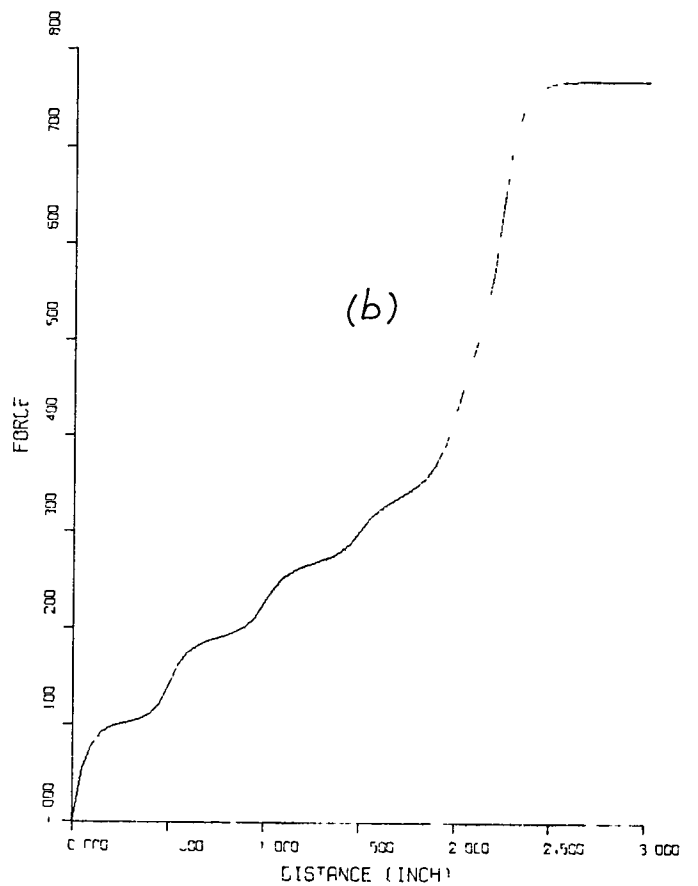


(d) STRESS IN AL. VS. DISTANCE

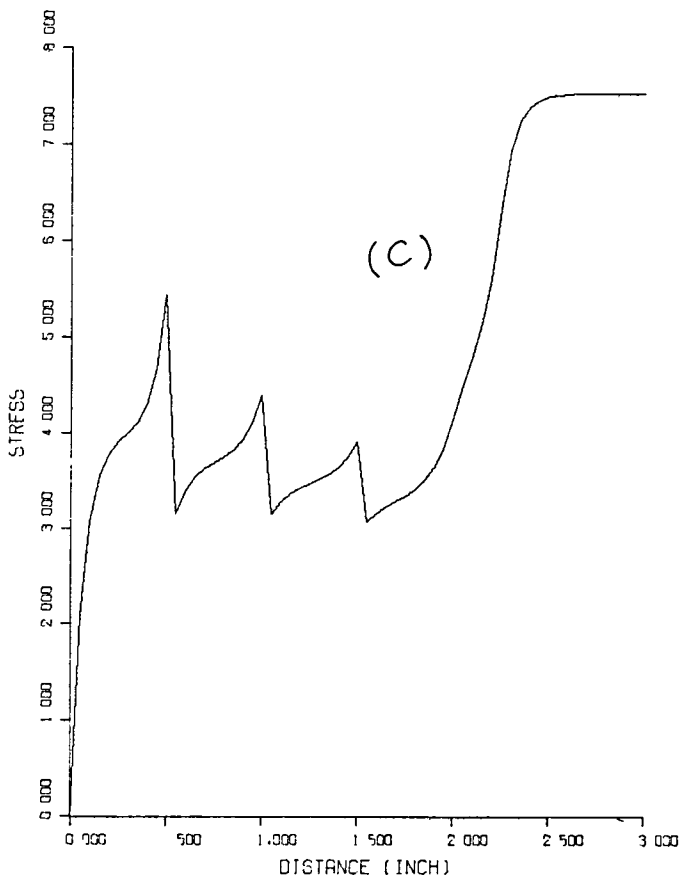
FIGURE 12 REINFORCED ALUMINUM-BORON EPOXY TUBE WITH $K_j = 0$, $h_3 = 0.001$ IN, $p_0 = 1$ (STEPS A)



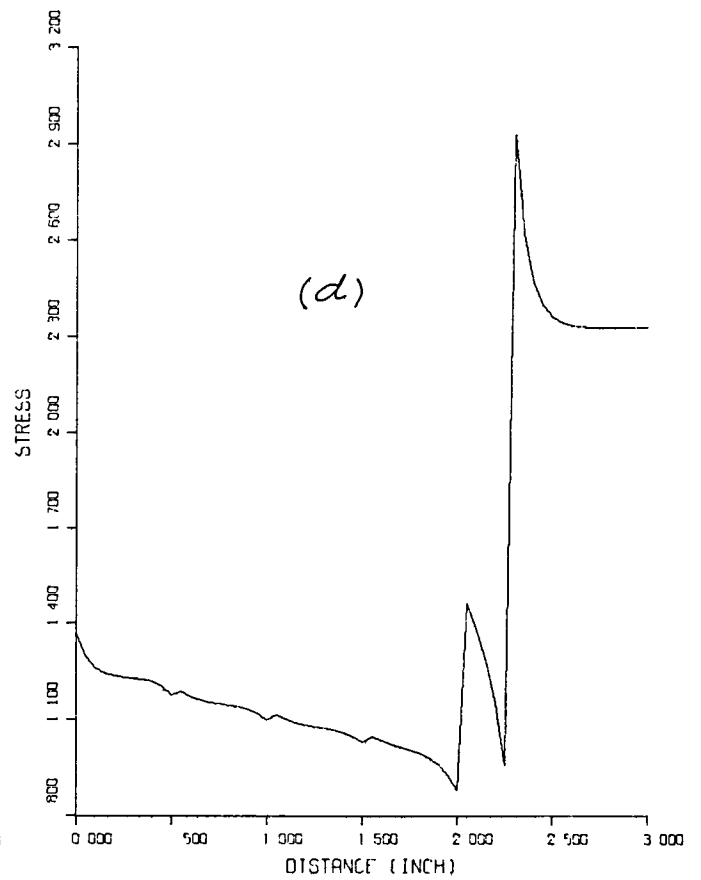
SHEAR STRESS VS. DISTANCE



FORCE IN B-E VS. DISTANCE

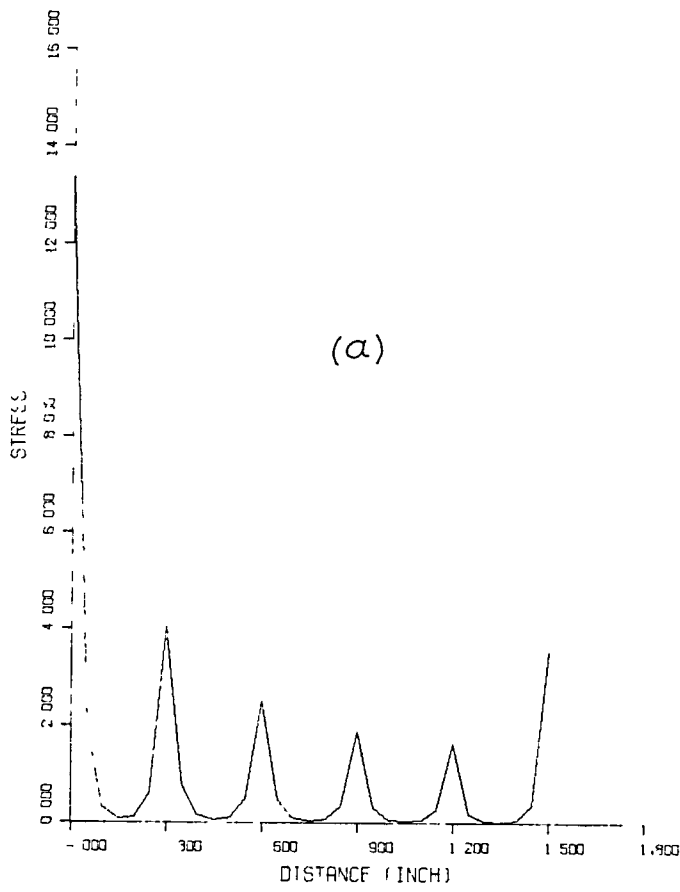


STRESS IN B-E VS. DISTANCE

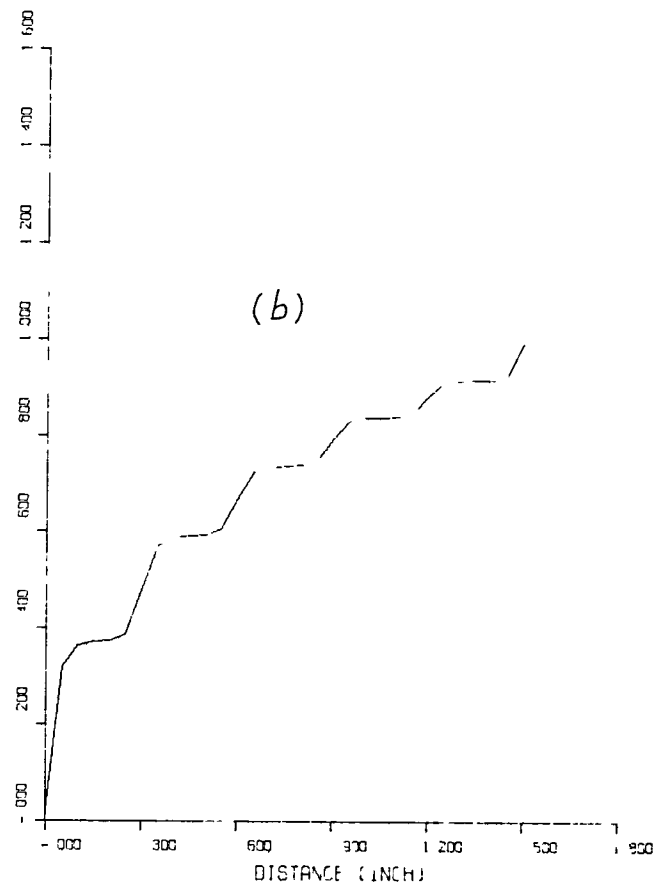


STRESS IN AL. VS. DISTANCE

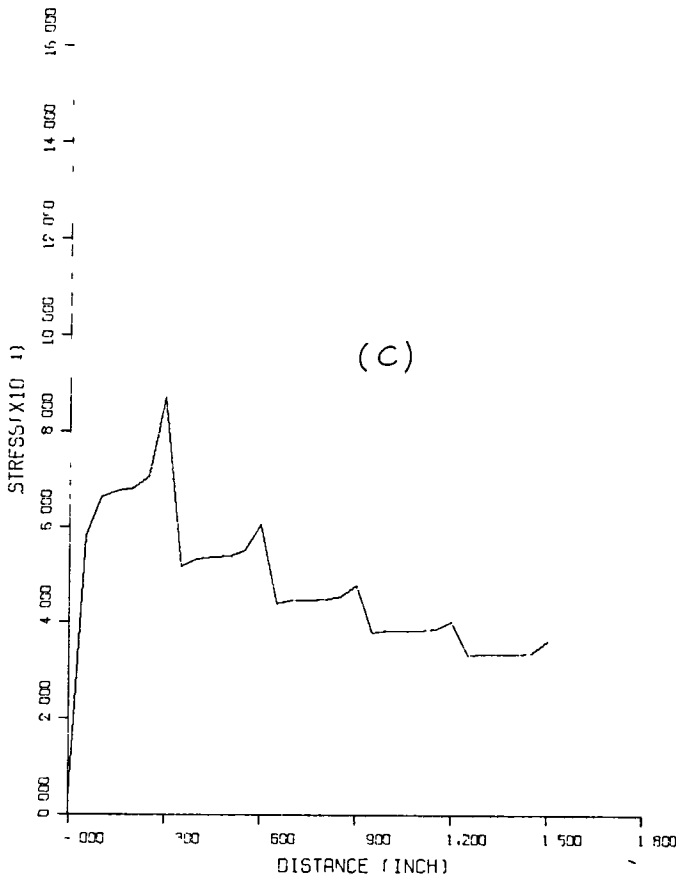
FIGURE 13 REINFORCED ALUMINUM-BORON EPOXY TUBE WITH $K_j = 0$, $h_3 = 0.001$ IN., $p_0 = 1$
(ALTERNATE STEPS B)



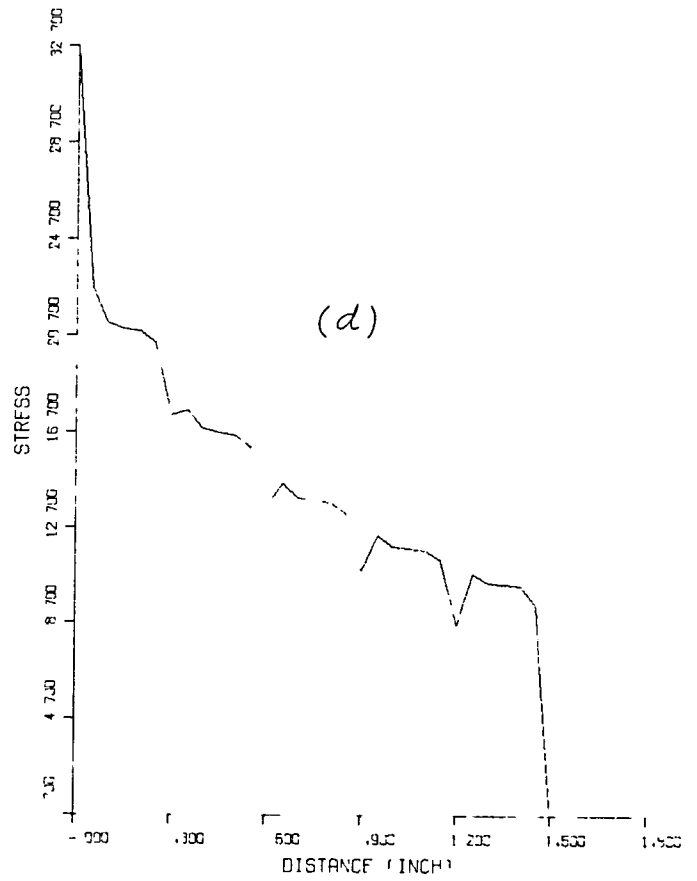
SHEAR STRESS VS. DISTANCE (L=0.3)



FORCE IN B-E VS. DISTANCE (L=0.3)

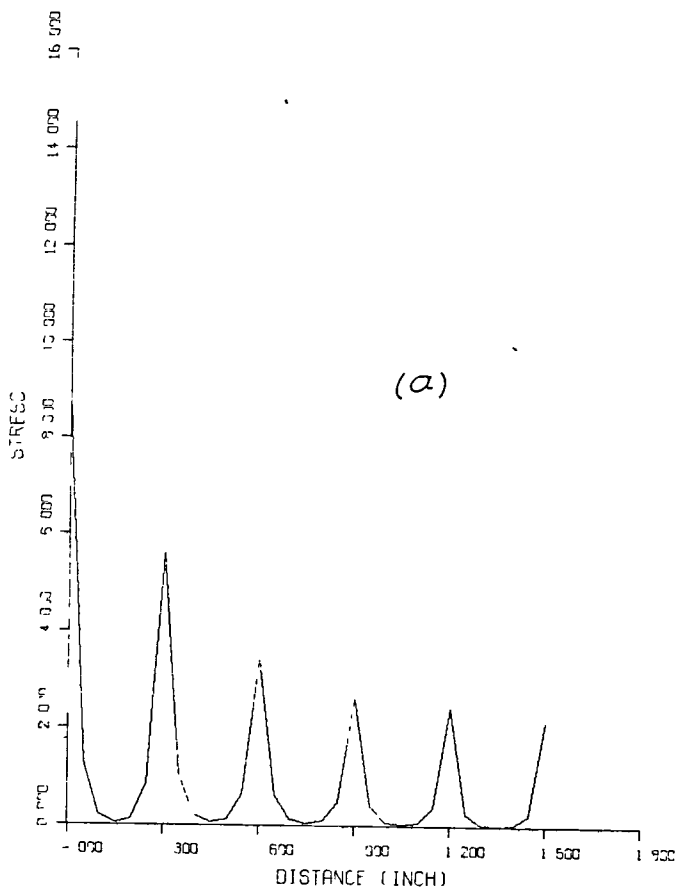


STRESS IN B-E VS. DISTANCE (L=0.3)

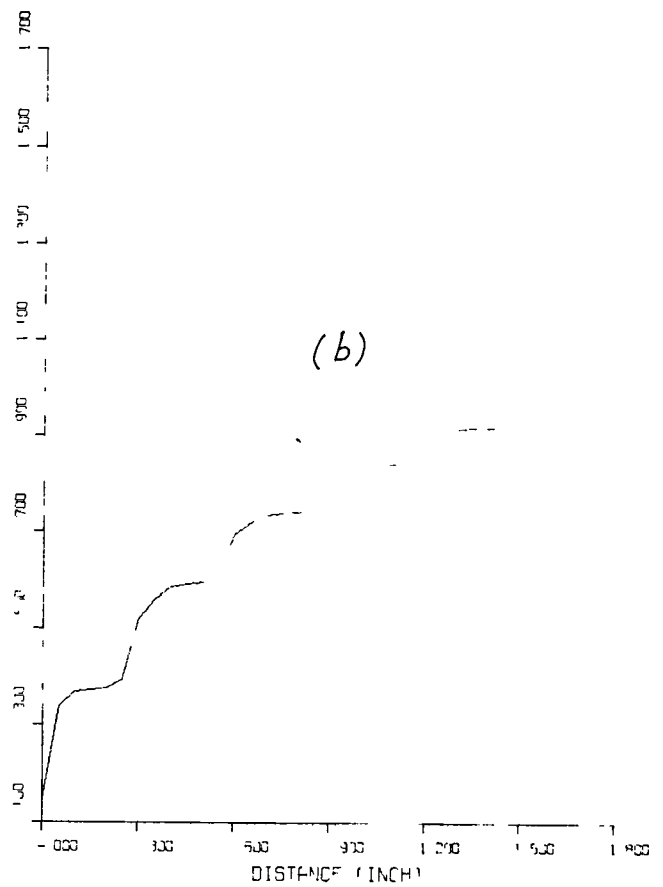


STRESS IN AL VS. DISTANCE (L=0.3)

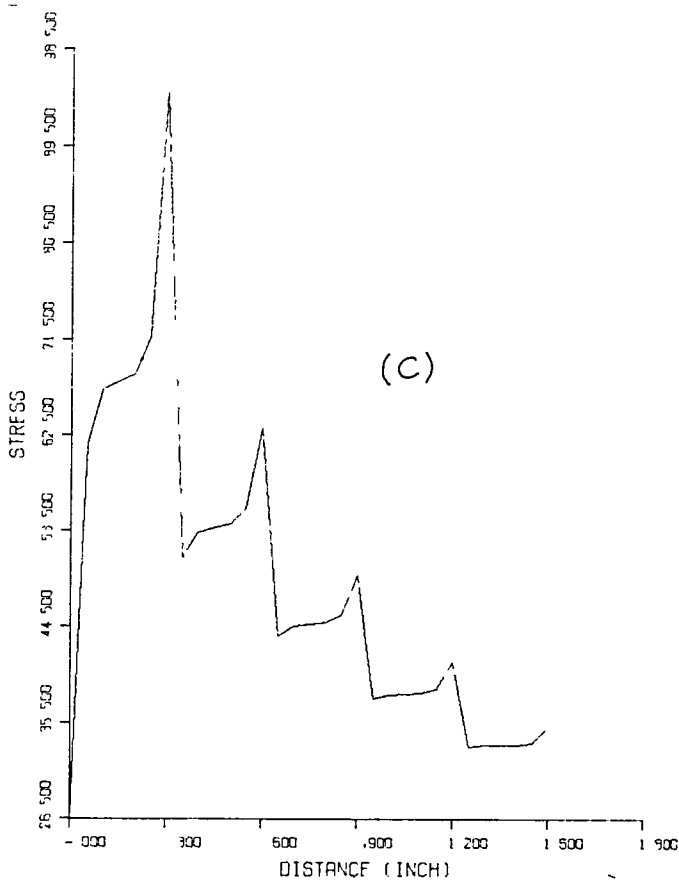
FIGURE 14 BONDED PLATES WITH $\bar{\sigma}_2 = 0$, $L = 0.3$ IN, $h_3 = 0.001$ IN, $d_3 = 0.01$ IN, $K_j \neq 0$, $p_0 = 1$



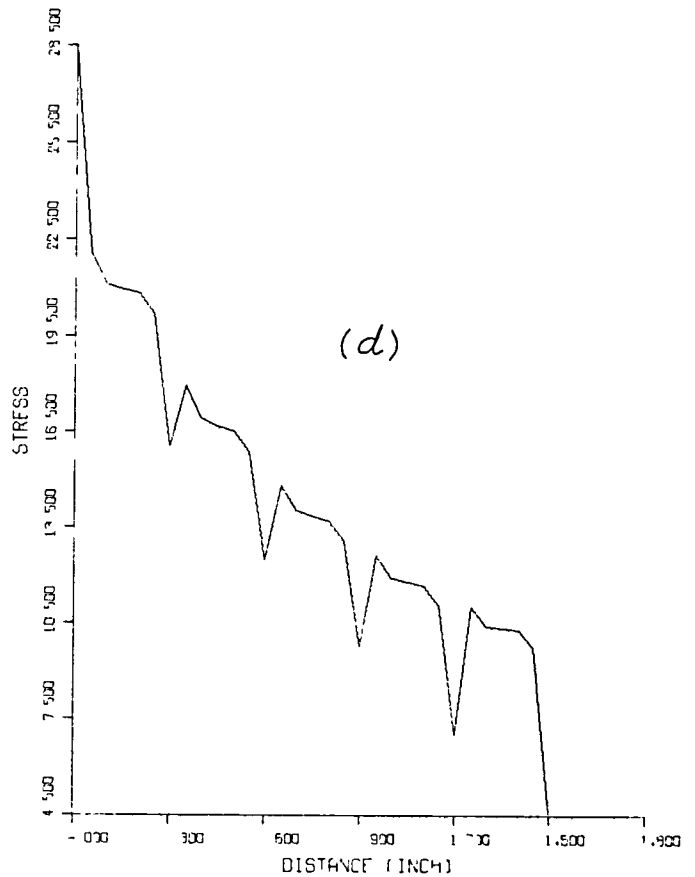
SHEAR STRESS VS. DISTANCE (L=0.3)



FORCE IN B-E VS. DISTANCE (L=0.3)



STRESS IN B-E VS. DISTANCE (L=0.3)



STRESS IN AL. VS. DISTANCE (L=0.3)

FIGURE 15 BONDED PLATES WITH $\bar{\sigma}_z = 0$, $L = 0.3$ IN, $h_3 = 0.001$ IN, $d_3 = 0.001$ IN, $K_f \neq 0$, $P_0 = 1$

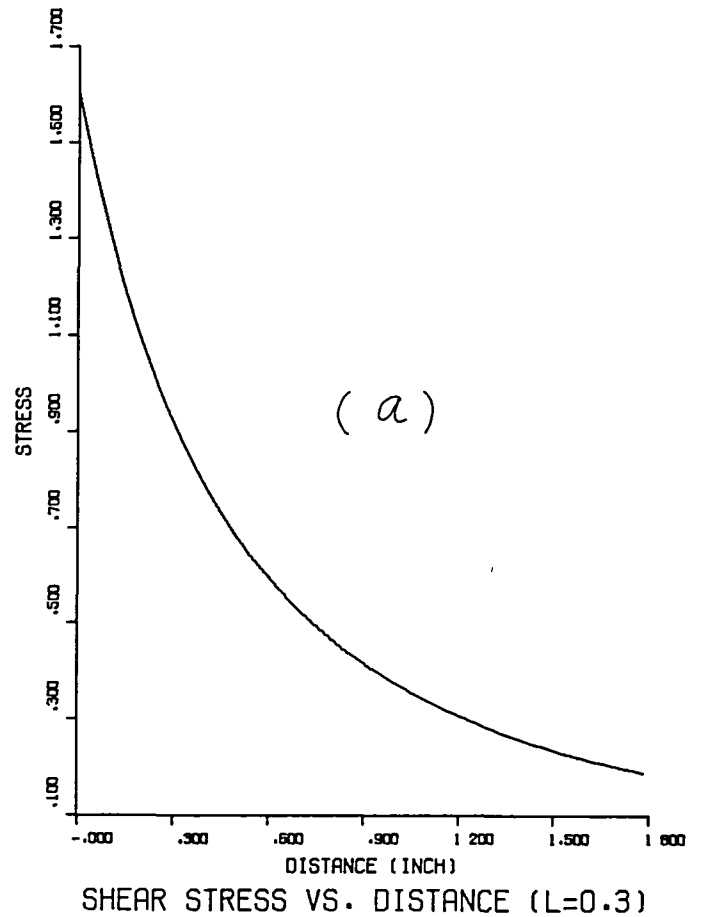
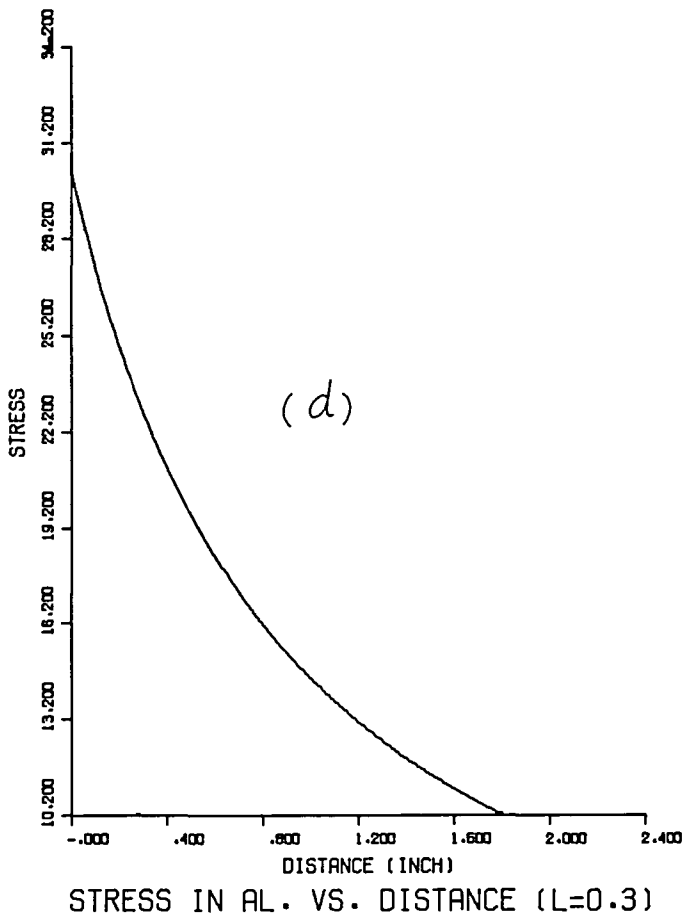
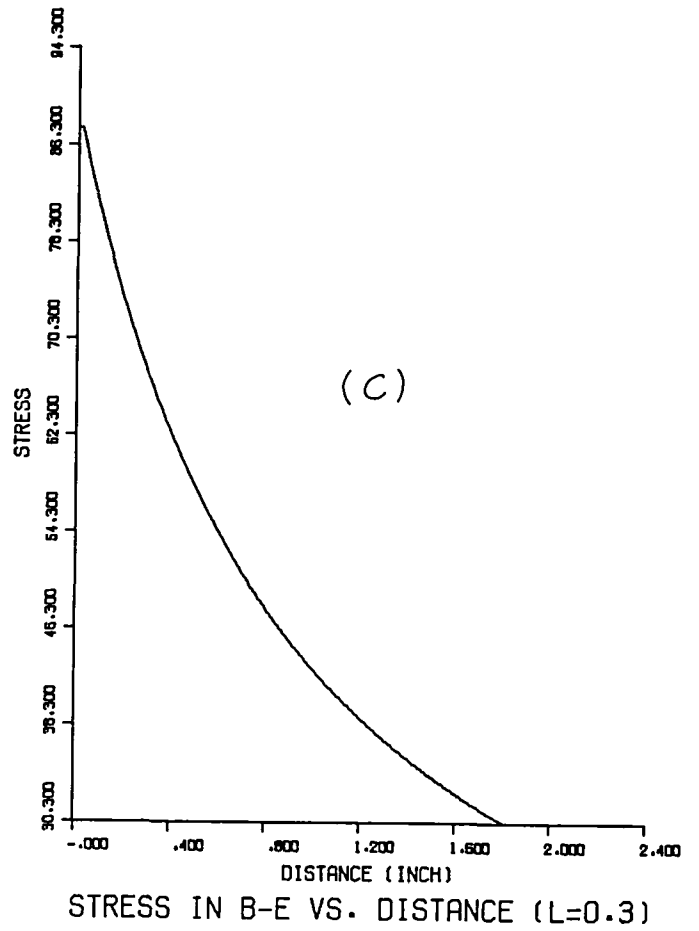
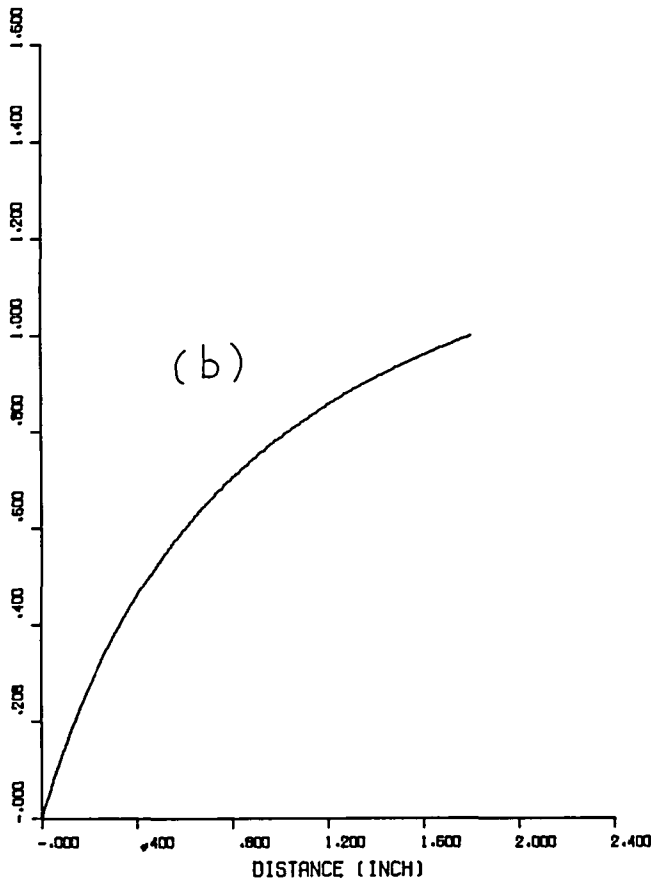


FIGURE 16 BONDED PLATES WITH A SMOOTHLY TAPERED JOINT, $\bar{\epsilon}_2 = 0$, $h_3 = 0.001$ IN, $l = 1.8$ IN, $p_0 = 1$

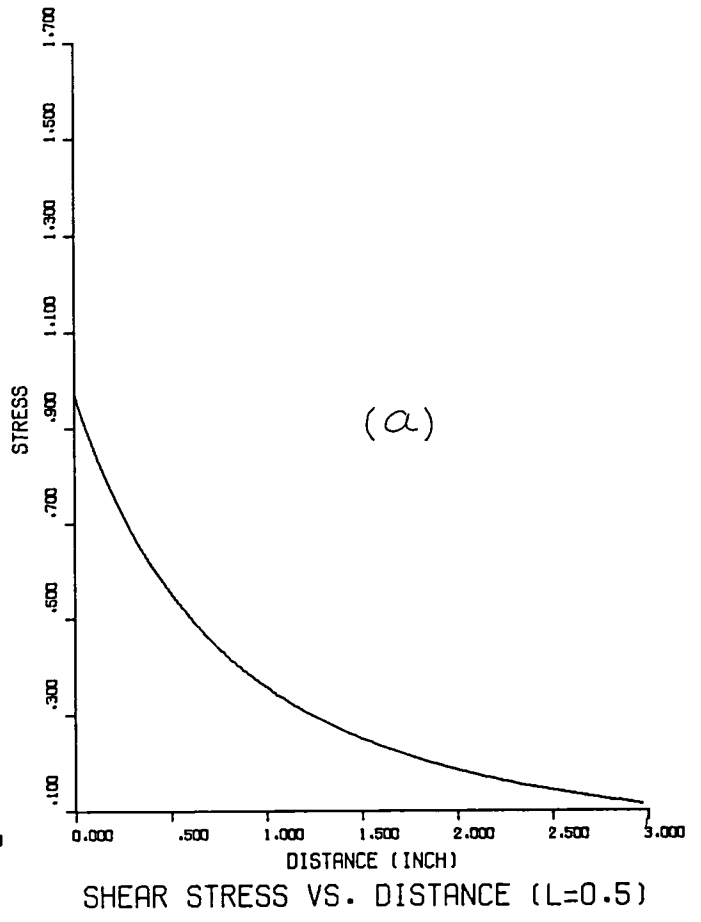
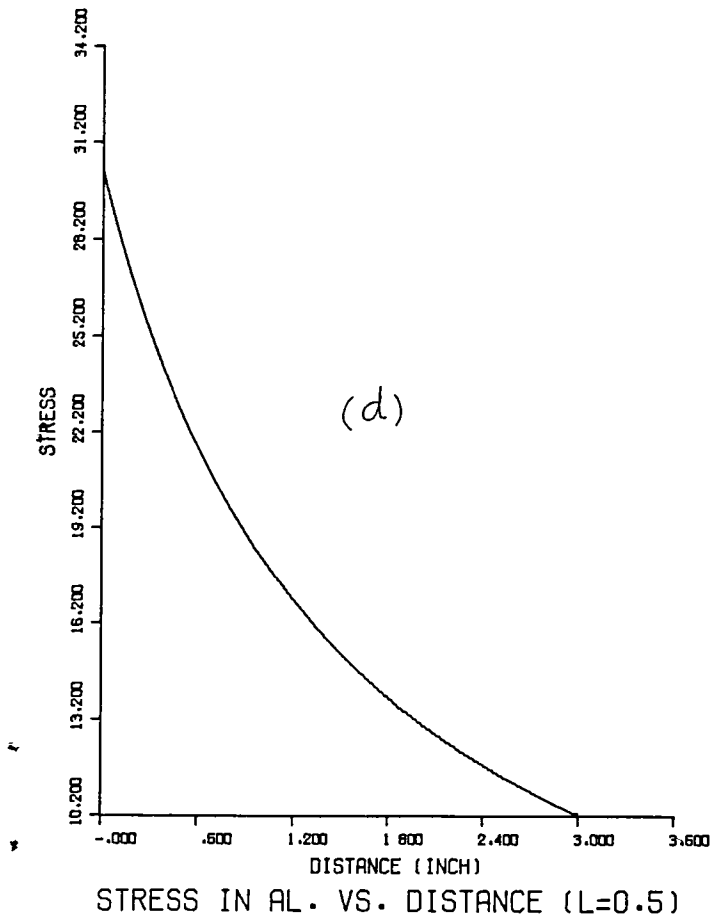
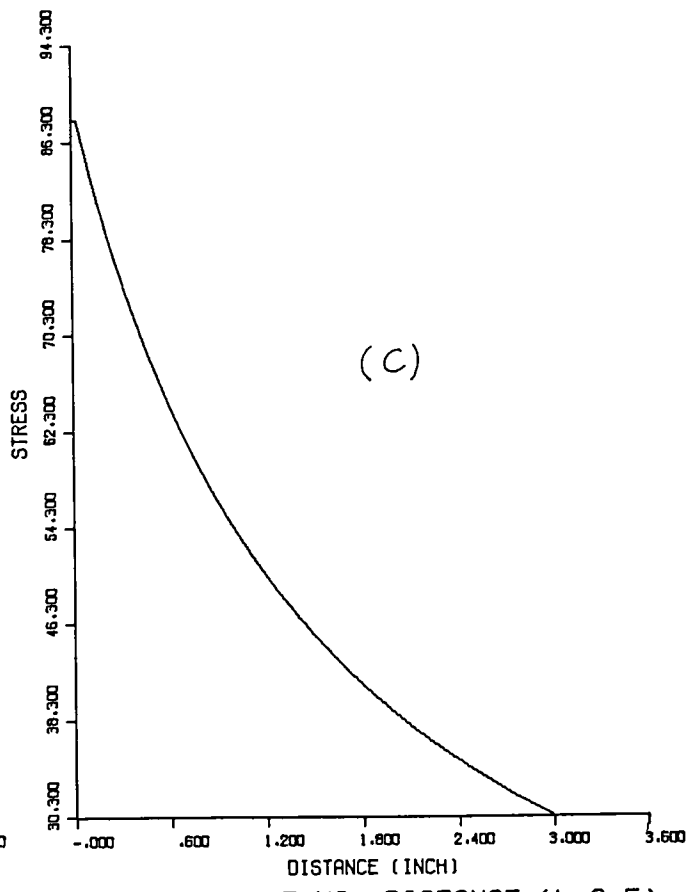
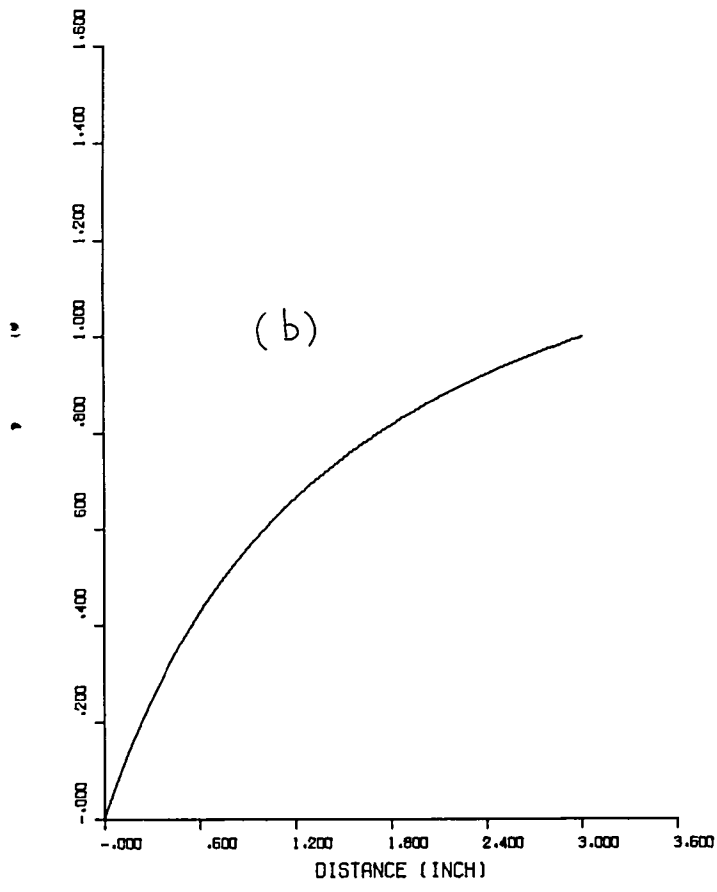


FIGURE 17 BONDED PLATES WITH A SMOOTHLY TAPERED JOINT, $\epsilon_2 = 0$, $h_3 = 0.001$ IN, $\lambda = 3.0$ IN, $p_0 = 1$

End of Document